UPPSALA
UNIVERSITET

Digital Comprehensive Summaries of Uppsala Dissertations from the Faculty of Medicine 812

Intensive Care Unit Muscle Wasting

Skeletal Muscle Phenotype and Underlying Molecular Mechanisms

SUDHAKAR REDDY AARE

ACTA
UNIVERSITATIS
UPSALIENSIS
UPPSALA
2012

ISSN 1651-6206
ISBN 978-91-554-8469-9
urn:nbn:se:uu:diva-180374

Dissertation presented at Uppsala University to be publicly examined in Hedstrandsalen, Ingang 70, bv Akademiska Sukhuset, Uppsala, Wednesday, October 24, 2012 at 13:15 for the degree of Doctor of Philosophy (Faculty of Medicine). The examination will be conducted in English.

Abstract
Aare, S. R. 2012. Intensive Care Unit Muscle Wasting: Skeletal Muscle Phenotype and Underlying Molecular Mechanisms. Acta Universitatis Upsaliensis. *Digital Comprehensive Summaries of Uppsala Dissertations from the Faculty of Medicine* 812. 66 pp. Uppsala. ISBN 978-91-554-8469-9.

Acute quadriplegic myopathy (AQM), or critical illness myopathy, is a common debilitating acquired disorder in critically ill intensive care unit (ICU) patients characterized by generalized muscle wasting and weakness of limb and trunk muscles. A preferential loss of the thick filament protein myosin is considered pathognomonic of this disorder, but the myosin loss is observed relatively late during the disease progression. In attempt to explore the potential role of factors considered triggering AQM in sedated mechanically ventilated (MV) ICU patients, we have studied the early effects, prior to the myosin loss, of neuromuscular blockade (NMB), corticosteroids (CS) and sepsis separate or in combination in a porcine experimental ICU model. Specific interest has been focused on skeletal muscle gene/protein expression and regulation of muscle contraction at the muscle fiber level. This project aims at improving our understanding of the molecular mechanisms underlying muscle specific differences in response to the ICU intervention and the role played by the different triggering factors.

The sparing of masticatory muscle fiber function was coupled to an up-regulation of heat shock protein genes and down-regulation of myostatin are suggested to be key factors in the relative sparing of masticatory muscles. Up-regulation of chemokine activity genes and down-regulation of heat shock protein genes play a significant role in the limb muscle dysfunction associated with sepsis. The effects of corticosteroids in the development of limb muscle weakness reveals up-regulation of kinase activity and transcriptional regulation genes and the down-regulation of heat shock protein, sarcomeric, cytoskeletal and oxidative stress responsive genes. In contrast to limb and craniofacial muscles, the respiratory diaphragm muscle responded differently to the different triggering factors. MV itself appears to play a major role for the diaphragm muscle dysfunction. By targeting these genes, future experiments can give an insight into the development of innovative treatments expected at protecting muscle mass and function in critically ill ICU patients.

Keywords: acute quadriplegic myopathy, gene expression, myosin, heat shock proteins, mechanical ventilation, myostatin, sepsis, corticosteroids, diaphragm

Sudhakar Reddy Aare, Uppsala University, Department of Neuroscience, Clinical Neurophysiology, Akademiska sjukhuset, SE-751 85 Uppsala, Sweden.

ISSN 1651-6206
ISBN 978-91-554-8469-9
urn:nbn:se:uu:diva-180374 (http://urn.kb.se/resolve?urn=urn:nbn:se:uu:diva-180374)

To my Family

List of Papers

This thesis is based on the following papers, which are referred to in the text by their Roman numerals.

I. **Aare S.,** Ochala J., Norman HS., Radell P., Eriksson LI., Göransson H., Chen YW., Hoffman EP., Larsson L. (2011) Mechanisms underlying the sparing of masticatory versus limb muscle function in an experimental critical illness model. *Physiol Genomics*, 43(24):1334-50.

II. **Aare S.,** Radell P., Eriksson LI., Chen YW., Hoffman EP., Larsson L. (2012) Role of sepsis in the development of limb muscle weakness in a porcine intensive care unit model. *Physiol Genomics*, 44: 865-877.

III. **Aare S.,** Radell P., Eriksson LI., Chen YW., Hoffman EP., Larsson L. (2012) Effects of corticosteroids in the development of limb muscle weakness in a porcine intensive care unit model. *Submitted*.

IV. Ochala J., Renaud G*., Llano Diez M*., Banduseela VC., **Aare S.,** Ahlbeck K., Radell PJ., Eriksson LI., Larsson L. (2011) Diaphragm muscle weakness in an experimental porcine intensive care unit model. *PLoS One* 6(6):e20558.

Out of the thesis

1. Liu JX, Höglund AS, Karlsson P, Lindblad J, Qaisar R, **Aare S**, Bengtsson E, Larsson L. Myonuclear domain size and myosin isoform expression in muscle fibres from mammals representing a 100,000-fold difference in body size. Exp Physiol. 2009 Jan; 94(1):117-29.
2. Ochala J, Gustafson AM, Diez ML, Renaud G, Li M, **Aare S**, Qaisar R, Banduseela VC, Hedström Y, Tang X, Dworkin B, Ford GC, Nair KS, Perera S, Gautel M, Larsson L. Preferential skeletal muscle myosin loss in response to mechanical silencing in a novel rat intensive care unit model: underlying mechanisms. J Physiol. 2011 Apr 15; 589(Pt 8):2007-26.
3. Banduseela VC., Chen YW., Göransson H., Norman HS., **Aare S.,** Radell P., Eriksson LI., Hoffman EP., Larsson L . Impaired autophagy, chaperone expression and protein synthesis in response to critical illness in porcine skeletal muscle. 2012. *Manuscript*.

Contents

Abbreviations

Activin-type II receptor B (ACVR2B)
Acute quadriplegic myopathy (AQM)
AMP-activated protein kinase (AMPK)
Autophagy lysosomal pathway (ALP)
Autophagy-related protein 7 (Atg7)
Bone morphogenic proteins (BMPs)
Chaperone mediated autophagy (CMA)
Corticosteroids (CS)
Compound muscle action potential (CMAP)
Creatine kinase (CK)
Critical illness myopathy (CIM)
Cross sectional area (CSA)
Direct muscle stimulation (DMS)
Eukaryotic initiation factor 2b (EIF2B)
Eukaryotic initiation factor 4E binding protein (4EBP1)
Forkhead box O (FoxO)
Glycogen synthase kinase 3 beta (GSK3β)
Heat shock proteins (HSPs)
Heat shock transcription factor (HSF-1)
Insulin-like growth factor 1 (IGF-1)
Intensive care unit (ICU)
Insulin receptor substrate (IRS)
Interleukin-6 (IL-6)
Intravenously (i.v.)
Mammalian target of rapamycin (mTOR)
Mitogen activated protein kinase (MAPK)
Matrix metalloproteinase-2 (MMP-2)
Mechanical ventilation (MV)
Monocyte chemoattractant protein 1 (MCP-1)
Muscle-specific RING finger protein 1 (MuRF1)
Myocyte enhancer factor 2 (MEF2)
Myosin binding protein (MyBP)
Myosin heavy chain (MyHC)
Myosin light chain (MyLC)
Neuromuscular blocking agents (NMBA)
Peroxisome proliferator-activated receptor gamma, coactivator 1 beta (PGC1β)

Phosphatidylinositol 3-kinase (PI3K)
Post-translational modifications (PTMs)
Reactive oxygen species (ROS)
Sensory nerve action potential (SNAP)
Signal transducer and activator of transcription 3 (STAT3)
Specific tension (ST)
Tissue inhibitor of metallo proteinases (TIMP 2)
Transforming growth factor-beta (TGF-β)
Ubiquitin (Ub)
Ubiquitin carboxyl-terminal hydrolase isozyme L3 (Uchl3)
Ubiquitin proteasome system (UPS)

Introduction

Skeletal muscle

Skeletal muscle is the most abundant and dynamic structure in the human body. Muscle fibers are the individual units of the skeletal muscle. The size and number of these fibers vary according to muscle type. Muscle fibers are packed in to small bundles of fibers, i.e., fascicles. The muscle fiber is made up of thousands of myofibrils arranged in parallel. The final functional unit in the myofibril is the sarcomere, containing the myosin and actin filaments (figure 1).

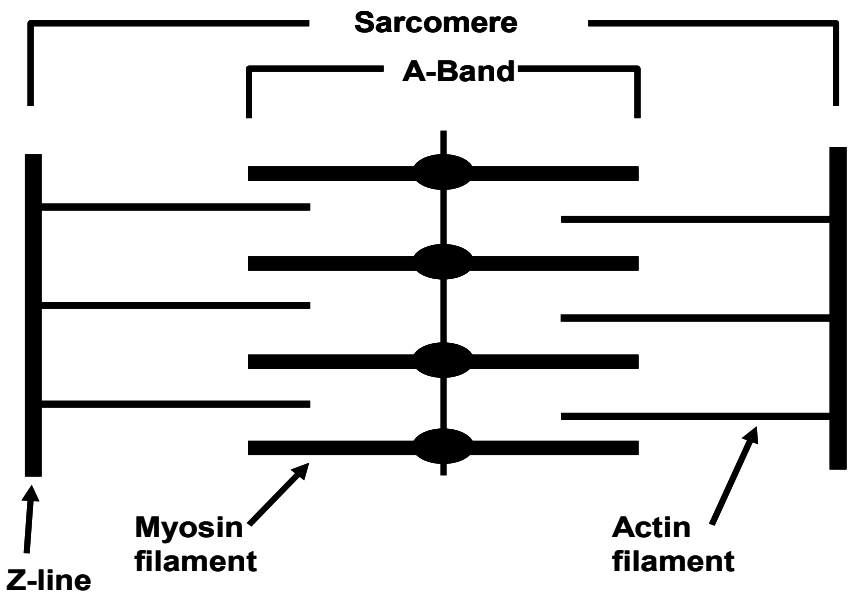

Figure 1. The structure of sarcomere. Each sarcomere is bounded by two Z lines. Within the sarcomere are the thick myosin filaments and thin actin filaments.

Myosin

Myosin is the molecular motor generating skeletal muscle contraction. The myosin molecule contains six proteins which forms a hexameric complex. The key nomenclature used to illustrate each of these six proteins is based on their molecular weights. The native myosin molecule constitutes of two myosin heavy chains (MyHCs) and each MyHC is coupled with one essential myosin light chain (MLC1 or MLC3) and one regulatory myosin light chain (MLC2). Each myosin heavy chain is made up of: 1) a long rod region; 2) sub fragment-2; S2); and 3) a globular head (also known as subfragment-1; S1) (figure 2).

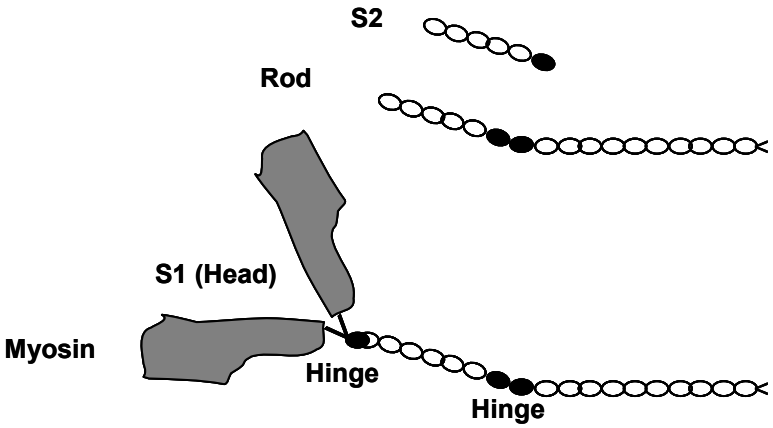

Figure 2. Structure of the myosin heavy chain. This diagram is obtained and adjusted from Biophysical journal Volume 90, Issue 8, 2006, Pages 2852–2866.

The MyHC rod region is important from a structural perspective because it determines the packing of MyHCs within the thick filament. In contrast, the globular head is directly implicated in binding to actin and generating force. The globular head consists of three domains known as: catalytic domain, converter domain and lever arm. The catalytic domain contains sites occupied with binding actin, binding ATP and hydrolyzing ATP. The converter region is presently thought to be involved in the transduction of energy, whereas the lever arm transports the load. Mutations in the globular head are supposed to play a key role in serious cardiomyopathies such as familial hypertrophic cardiomyopathy. Each MyHC has one essential and one regulatory light chain bound to the S1 fragment (17, 107, 123)

The diversity of the native myosin molecule is complicated by the presence of different isoforms, in both the MyHC and MLCs. From a mechanical viewpoint, muscles could be categorized as slow and fast. In the past 20 years, it has been revealed (at various levels) that the speed related properties of skeletal muscle are due primarily to the existence of different MyHC isoforms, and that the kinetics of cross bridge cycling can be modulated by MLC isoforms (67, 70). The different fiber types are used to classify and linked to the MyHC isoform composition of the fiber. The ultimate design constriction of skeletal muscle is the force-velocity relationship and the shape of this association is dependent on the kinetics of cross bridge cycling In small adult mammals, the primary MyHC isoforms found in most muscles is the slow type I, fast type IIa, IIx, and IIb MHC isoforms (in order of their ATPase activity). In humans, it is presently thought that only the first three MyHC isoforms are expressed. Additional adult MyHC isoforms have been found in muscles from the larynx (Type IIL), mastication (superfast type IIM), and that are involved in the movement of the eyes (EO). Furthermore two developmental MyHC isoforms have been found in mammalian skeletal muscle, these are referred to as the embryonic (E) and neonatal (NEO) MyHC isoforms. Finally, the hearts of both small mammals and humans are known to express two cardiac isoforms, the β- (type I) and α-cardiac MyHC isoforms.

Actin

In skeletal muscle, actin is a 42 kDa protein. The sarcomere is composed of filamentous actin polymers (F-actin) that regularly interact with the myosin heads to produce contractile force (55). Actin is extremely preserved with only 23 out of 375 residues differing between skeletal muscle and a non-muscle source. In sarcomeric muscle both α-skeletal and α-cardiac actin are expressed (122). Additionally, actin has been reported to have a two-fold longer turnover rate compared to the myosin (72, 85).

Muscle contraction

Myosin and actin are the two key molecules involved in the muscle contraction. During contraction, actin filaments (thin filaments) and myosin filaments (thick filaments) slide past one other, known as the sliding filament theory.

According to the cross bridge theory, cross bridges extend from the myosin filament interact cyclically in a rowing motion with the actin filament, as ATP is hydrolyzed. The actomyosin interaction is initiated by a weak electrostatic bond between positively charged myosin and negatively charged actin molecules. Consequently, actin driven ATP hydrolysis leads to a strong binding state parallel to a lever arm movement of the myosin head (112). This is followed by the release of ADP; and substituted by ATP, the S1 segment dissociates from actin. The myosin filament remains stationary throughout the contraction with each cross bridge acting as a force generator. The number of cross-bridges and the force generated per cross bridge determines the force generated by the muscle fiber (86, 92).

Regulation of muscle mass

Protein degradation and synthesis are the two components regulating skeletal muscle size. Muscle hypertrophy is the result of synthesis exceeding degradation and atrophy the opposite.

Protein synthesis

Skeletal muscle protein synthesis occurs via various signaling pathways such as myostatin, the negative regulator of the skeletal muscle size, has been implicated in different hypertrophy models. Myostatin inhibits activation of the Akt/mammalian target of rapamycin (mTOR)/p70S6 protein synthesis pathway, which mediates both differentiation in myoblasts and hypertrophy in myotubes (142). Insulin-like growth factor 1(IGF-1) is a protein growth factor that has been demonstrated to be sufficient to induce skeletal muscle hypertrophy by stimulating the phosphatidylinositol-3 kinase (PI3K)/Akt pathway, resulting in the downstream activation of targets which are required for protein synthesis (12, 114). Glycogen synthase kinase 3 beta (GSK3β) is another substrate of Akt that has been shown to modulate hypertrophy. Expression of a dominant negative, kinase inactive form of GSK3β induces hypertrophy in skeletal myotubes (114), as pharmacologic inhibition of GSK3β (147) (figure 3).

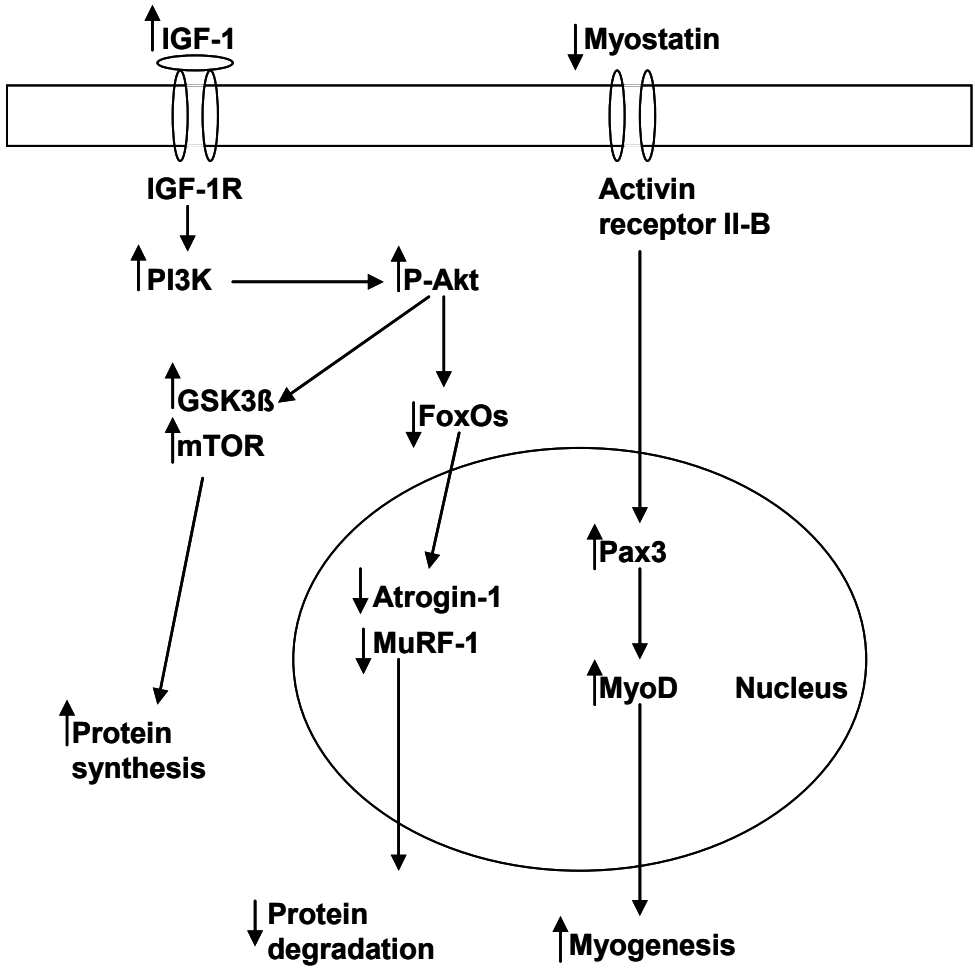

Figure 3. The function of IGF-1 and Myostatin in skeletal muscle protein homeostasis. This diagram is obtained and adjusted from Kidney International (2008) 74**,** 180–186.

Protein degradation

The degradation of proteins in the cell is critical for intracellular signaling and cell division. However, abnormal protein degradation results in muscle wasting. The major protein degradation mechanisms observed in skeletal muscle are the ubiquitin proteasome system (UPS), autophagy lysosomal pathway (ALP) and calpain mediated protein degradation pathways.

Proteins are continuously synthesized and degraded in skeletal muscle. Cells which are subject to stress such as starvation, heat-shock, chemical insult or mutation respond by increasing the rates of proteolysis. For exam-

ple, oxidative stress has been shown to damage a variety of proteins and target them for rapid degradation. Post translational protein modifications also play an important role for protein degradation

Ubiquitn proteasome system

The ubiquitin proteasome pathway, preserved from yeast to mammals, is essential for the targeted degradation of most short-lived proteins in the eukaryotic cell. Targets include cell cycle regulatory proteins, whose timely degradation is vital for controlled cell division, as well as proteins unable to fold properly within the endoplasmic reticulum. Ubiquitin (Ub) is a small protein that is composed of 76 amino acids. This protein is found only in eukaryotic organisms. Among eukaryotes, ubiquitin is highly conserved. For example, there are only three differences in the sequence of Ub from yeast compared with human Ub. The UPS system contains three different types of enzymes; E1 enzymes known as Ub-activating enzymes, E2 enzymes known as Ub-conjugating enzymes and E3 enzymes known as Ub-ligases which guide the protein for degradation. Ub itself does not degrade proteins; it serves only as a tag that marks proteins for degradation. The degradation is carried out by the 26S proteasome (figure 4).

In skeletal muscle atrophy, the two muscle specific E3 ubiquitin protein ligases Atrogin-1 and MuRF1 are markedly up regulated (11). MuRF1 and Atrogin-1 mediate atrophy by ubiquitinating particular protein substrates, causing them to undergo degradation by the proteasome. MuRF1's substrates include several components of the sarcomeric thick filament, including MyHCs (21). FOXO (fork head) family of transcription factors induces Atrogin-1 and FOXO3 activation was demonstrated to be sufficient to induce atrophy (120). Additionally it has been shown that NFkB activation induces atrophy in part through transcriptional up regulation of MuRF1 (16) and furthermore that P38 is another trigger for the up regulation of Atrogin-1 (82). Protein quality control needs the UPS to degrade misfolded or damaged proteins.

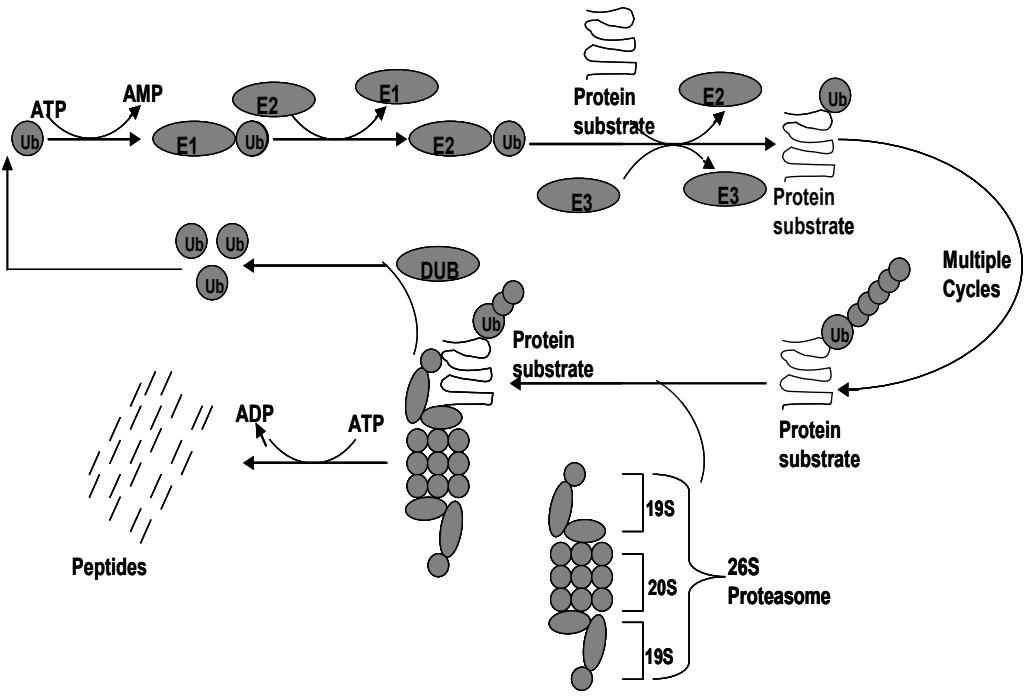

Figure 4. The ubiquitin/proteasome pathway. Multiple ubiquitination cycles resulting in a polyubiquitin chain are required for targeting a protein to the proteasome for degradation. The multisubunit 26S proteasome recognizes, unfolds and degrades polyubiquitinated substrates into small peptides. This diagram is obtained and adjusted from Cell Signaling Technology.

Autophagy lysosomal pathway

In eukaryotes, the lysosomal pathway degrades and recycles various cellular components by means of a process known as autophagy. Autophagy is a highly regulated homeostatic degradative process in which cells destroy and recycle their own components via the lysosomal machinery. In mammalian cells, autophagy is believed to occur at basal rates. There are three main forms of autophagy; microautophagy, macroautophagy and chaperon mediated autophagy (CMA) (60). In micro and chaperon mediated autophagy there is direct involvement of the lysosomes, which either engulfs small portions of the cytosol or receives chaperon mediated cargoes. Macroautophagy is a highly conserved homeostatic program for the degradation of cytoplasmic components including damaged organelles, toxic protein aggregates and intracellular pathogens (97) (figure 5).

Excessive activation of autophagy can lead to muscle wasting, however on the other hand, inhibition of lysosomal dependent degradation leads to myopathies like Pompe or Danon disease (79). Furthermore, the muscle specific Atg7 knock out induced autophagy inhibition results in muscle atrophy,

loss in force production and morphological features of myopathy (87). Skeletal muscles of collagen VI knockout mice have impaired autophagy and myofiber degeneration. Activation of autophagy by means of genetic, dietary and pharmacological approaches restored myofiber survival in the collagen VI knockout mice (47). Cathepsins are the main players in the ALP systems, they have been shown to be implicated in muscle wasting conditions including muscular dystrophies, sepsis, disuse atrophy, fasting and glucocorticoid induced atrophy (10). The most potent autophagy inhibitor in skeletal muscles is the kinase Akt. Excessive autophagy is detrimental to muscle mass and impaired autophagy can lead to many different debilitating myopathies. However an optimum ALP is essential for tissue homeostasis.

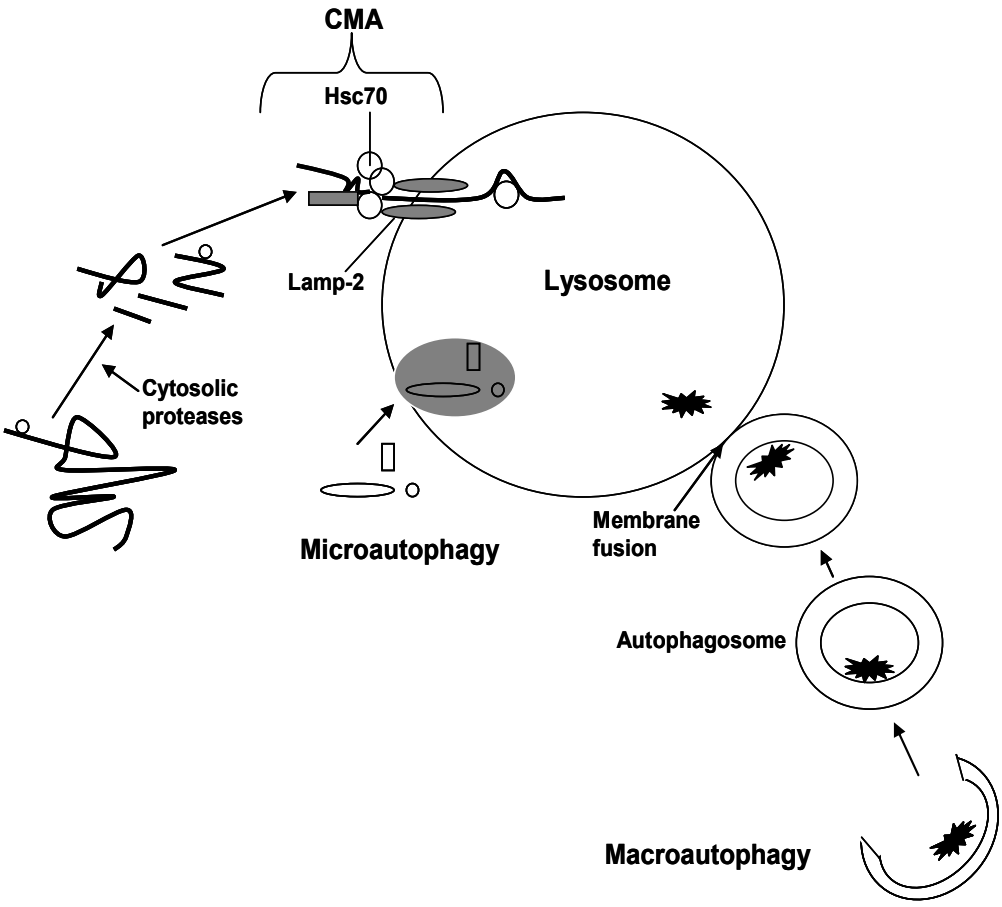

Figure 5. Different pathways of protein degradation in lysosomes. In microautophagy, portions of the cytosol are constantly internalized via lysosomal invaginations. In macroautophagy, the cytoplasm is sequestered into double-membrane structures, known as autophagosomes, which fuse with lysosomes. In CMA, specific cytosolic proteins are transported into lysosomes via a molecular chaperone/receptor complex composed of hsc70 and lamp-2. Cytoplasmic antigens may first be processed by cytosolic proteases before transport to lysosomes. This diagram is obtained and adjusted from PNAS 2005 vol. 102 no. 22 7779-7780.

Calpain mediated protein degradation

The intracellular calcium-dependent proteases (calpains) and their endogenous protein inhibitor (calpastatin) are present in many different mammalian cells. Muscle tissue mainly expresses three different types of calpains: the ubiquitous calpains 1, 2 (mu and m) and muscle specific calpain 3 (p94). The calpain system performs a broad spectrum of physiological functions, including proteolysis of proteins involved in the cell cycle, apoptosis, cytoskeleton organization and signal transduction (41) (figure 6).

Most of the limb-girdle muscular dystrophies are myopathies which are caused by gene mutations which affect structural proteins. However, LGMD2A is caused by mutations affecting the capn3 gene coding for the skeletal muscle specific calpain 3 (113). Oxidation increases the susceptibility of skeletal muscle myofibrillar proteins to degradation by the calcium-activated proteases calpain 1 and calpain 2 (135). Several studies have recognized that calpains are elevated in atrophic conditions like disuse, denervation, glucocorticoid treatment and sepsis (48). There are reports suggesting that calpain 3 exerts a protective effect against atrophy by directing the NFκB pathway towards an anti apoptotic response as well as having a number of links with proteasome activity. Deficiency in calpain 3 leads to a muscular dystrophy phenotype, demonstrating that its activity is necessary for skeletal muscle homeostasis. (9).

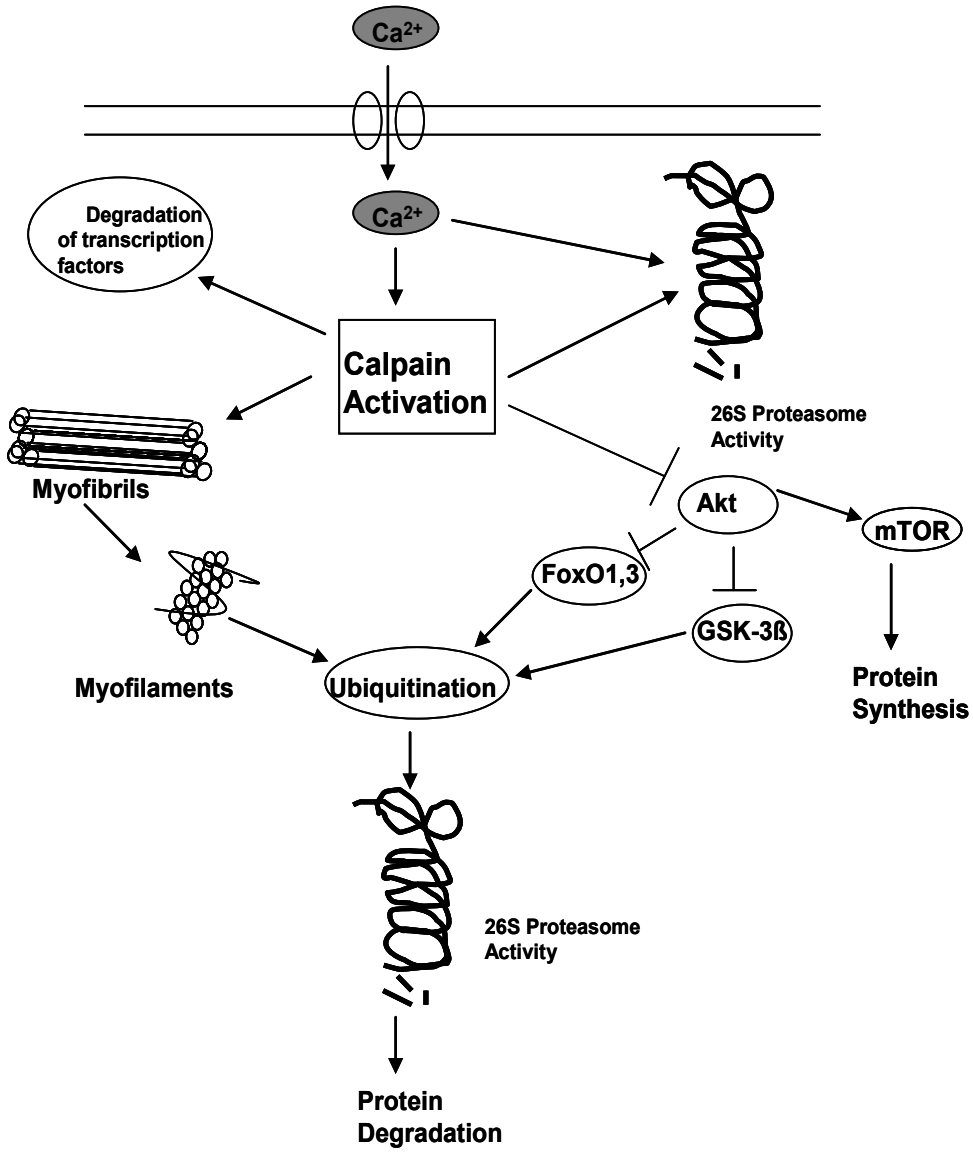

Figure 6. Summary of calpain activation in skeletal muscle wasting conditions. Calpains are activated by calcium, although other mechanisms are also contributing to calpain activation. The most significant muscle wasting-related consequence of calpain activation is cleavage of the myofibrillar cytoskeletal proteins, resulting in the disruption of the sarcomere and release of myofilaments that are subsequently ubiquitinated and degraded by the 26S proteasome. This diagram is obtained and adjusted from AJP - Endo 2008 vol. 295 no. 4 E762-E77.

Gene profiling

Gene profiling is an outstanding tool to identify genetic mechanisms, networks, molecular pathways involved in the skeletal muscle development and disease. The following gene groups are involved in skeletal muscle regulation in the porcine ICU model, i.e., in response to different triggering factors as well as muscle type specific differences.

Transcription factors

Different transcription factors will activate in skeletal muscle in response to mechanical ventilation, sedation, immobilization, neuro muscular blockers, corticosteroids and sepsis in combination or separately. These include runt-related transcription factor (RUNX1) associated with preventing atrophy and myofibrillar disorganization (145); ID1 and ID2 (inhibitor of differentiation), members of the helix-loop-helix (HLH) protein family, dimerise with basic HLH transcription factors. These proteins inhibit E-box mediated gene expression by forming nonfunctional complexes with myogenic bHLH factors such as *myoD* and *myogenin* during differentiation (65);

Early growth response 1 (EGR1), a transcriptional regulator that activates transcription of target genes whose products are involved in regulation of cell growth and differentiation (36); activator protein 1 (Ap-1), the inducible transcriptional complex composed of proto-oncogene c-Fos (FOS) and proto-oncogene c-Jun (JUN) and these oncogenes have been implicated as regulators of cell proliferation, differentiation and transformation; insulin-like growth factor 1 receptor (IGF1R) plays an important role in normal and regenerating muscle tissue establishment and maintenance of mature muscle phenotype (35); T-box- containing transcription factor (Tbx1) is required for transcriptional activation of the myogenic determination of genes in the mandibular arch (59). Tbx1 acts by activating core myogenic program of pharyngeal muscles and synergistically with *Myf5* upstream of *myoD* in the pharyngeal arch (118).

Myostatin is the negative regulator of the skeletal muscle growth and it is a member of the transforming growth factor-beta (TGF-β) super family. Blocking of the myostatin signal transduction pathway by specific inhibitors and genetic manipulations lead to muscle hypertrophy and hyperplasia (94); activin-type II receptor B (ACVR2B) and follistatin are the two important myostatin-related genes involved in the regulation and signaling of myostatin. Myostatin inhibits protein synthesis and satellite cell function in skeletal muscle and myostatin negatively regulates the activation of satellite cells and myostatin knockout mice have increased satellite cell activation (91).

The transcriptional factors which are involved in the myogenesis includes jun B proto-oncogene (JUNB) promotes muscle growth independent of the AKT pathway (111); signal transducer and activator of transcription 3 (STAT3) involved in myogenic differentiation (144); basic helix-loop-helix

family member e40 (BHLHB2), inhibiting the expression of different muscle regulatory factors (75); myocyte enhancer factor 2A (MEF2A) is a transcription factor that is a critical regulator of structural and contractile proteins and plays a role in skeletal muscle myogenesis. In hibernating ground squirrels MEF2A gene and protein levels are positively regulated and help in the muscle remodeling (140); and V-maf musculoaponeurotic fibrosarcoma oncogene homolog G (MAFG) gene acts as a transcriptional repressor when they dimerize. If they dimerize with other basic- zipper proteins then they serve as transcriptional activators. MAFG acts as a binding partner for the nuclear factor erythroid 2-related factor 2 (NRF2), in hibernating ground squirrels both MAFG and NRF2 transcripts were up-regulated in heart muscle in order to prevent the oxidative stress (100).

Some transcription factors are involved in muscle regulation which include Kruppel-like factor 11 (KLF11) also known as transforming growth factor-beta-inducible early growth response protein2 (TIEG2) and is a family of primary response genes induced by TGF-beta, which are well recognized in regulating cellular proliferation and apoptosis (58); transducin like enhancer split 1 (TLE1) is a transcriptional co-repressor of basic helix-loop-helix proteins (50) known to inhibit the expression of diverse muscle regulatory factors, and the SLC2A4 regulator essential for normal GLUT4 expression and transcriptional regulation via an AMPK-induced mechanism (52).

Heat shock proteins (HSPs)

HSPs are involved in the protection of proteins in response to heat stress, oxidative stress and ischemia. In addition, HSPs are also involved in different physiological functions. These proteins are primarily involved in protein folding, synthesis and chaperone function of misfolded proteins. Heat shock transcription factor (HSF-1) is one of the well-characterized heat shock transcription factors that are involved in acute stress. The high molecular-weight family of proteins include: HSP 110, HSP 90, HSP 70 and HSP 60. The lower molecular-weight family of proteins include: HSP 27 and alpha crystalline family. Ubiquitin C-terminal hydrolases (UCHs) constitute a subfamily of de-ubiquitinating enzymes that belongs to the cysteine proteases. Skeletal muscles of Uchl3 knockout mice show up-regulation of various heat shock proteins including HSP 27, HSP 40, HSP 70, HSP 90, and HSP 110. These results reveal that the skeletal muscle of Uchl3 knockout mice is under persistent stress and show cellular stress responses (128).

When tissues are challenged, HSPs will play a role by preventing inappropriate protein aggregation and mediating transport of immature or misfolded proteins to cell organelles for repair, packaging, or degradation. Increased HSP 90 expression has been shown in the regenerating muscle fibers of idiopathic inflammatory myopathies (25). HSP 70 has been reported involved in FOXO signaling, in disuse condition of rat soleus muscle. Up-regulation of HSP 70 prevent muscle atrophy (126) and HSP 70 over expres-

sion leads to protection against fatigue induced muscle injury (103). HSP 27 is a cytoprotective protein that is ubiquitously expressed in most cells, and is up-regulated in response to cellular stress. HSP 27 is a negative regulator of NFkB in skeletal muscle and is sufficient to inhibit MuRF1 and Atrogin-1 to attenuate skeletal muscle disuse atrophy (28).

αB-crystallin is a small heat shock protein (20 kDa) and is the well known stabilizer of intermediate filaments (27) and actin (132). It maintains cytoskeleton integrity, by acting as a chaperone for desmin (40). The αB-crystallin was up-regulated during muscle differentiation and mice lacking αB-crystallin die prematurely with extensive muscle wasting and it plays an important role in muscle homeostasis (133). DNAJA1 (HSP 40), a co-chaperone for the HSP 70 and stimulate ATPase activity. Heat shock factor 2 (HSF2), encodes a protein which is implicated in early stages of skeletal muscle regeneration (90). All together these heat shock proteins play a very important role in the sparing of the skeletal muscle in different conditions.

Sarcomeric protein

The regulatory thin filament protein tropomyosin β expressed in muscle fibers of the slow-twitch type. Myosin light chain kinase (MyLC-K) is a critical component in signaling sequences and involved in protein-protein interactions. Myosin heavy chain 7, cardiac muscle beta (MYH7) expressed in skeletal muscle tissues rich in slow-twitch type I muscle fibers and involved in the muscle contraction. Titin-cap (TCAP) also known as telethonin functions as a muscle assembly regulatory factor. Tropomyosin 3 (TPM3), gene binds to actin filaments in muscle and non-muscle cells. It plays a role, in association with the troponin complex, in the calcium dependent regulation of vertebrate striated muscle contraction. Myosin binding protein C1 (MyBP-C1) is the next to myosin most abundant protein in the thick filament and is suggested to play both an important structural and regulatory role in muscle contraction.

Oxidative stress responsive

Skeletal muscle is prone to oxidative stress due to various reasons and in order to protect muscle from stress different oxidative stress responsive genes were up-regulated which include thioredoxin (TXN) implicated in redox regulation of transcription factor NFkB in cell culture (51) and the cytosolic mammalian thioredoxin, has various functions in protection against oxidative stress (6). Peroxisome proliferative activated receptor gamma, co-activator beta (PPARGC1B or PGC-1β) gene implicated in mitochondrial biogenesis (5). Mitochondrial superoxide dismutase 2 (SOD2) protects the mitochondrial matrix by removing excessive superoxide anion (O_2^-) at the protein level.

Cell cycle

Various cell cycle regulation genes were altered including the cyclin/cyclin dependent kinase (CDK) inhibitor p21 which is involved in myogenic progenitor cell coordinated regulation of cell cycle exit and myogenic differentiation (49); death effector domain containing (DEDD) gene plays a role in inhibition of cyclin-dependent kinase-1 (Cdk1) function and it forms complexes with Akt and HSP90 and supports the stability of their function (61); diablo homolog (DIABLO) gene encodes an inhibitor of apoptosis protein (IAP)-binding protein and in denervated rat gastrocnemius muscle an increased expression was associated with DIABLO, leading to apoptosis in this atrophy model (134); Cofilin 2 (CFL2), an actin binding protein reported down-regulated in damaged muscle tissue (141) and met proto-oncogene (MET) is a skeletal muscle satellite cell marker (83).

Immune response

Complement component 7 (C 7) reported to play a key role as a major mediator of the direct tissue damage caused by complement activation. It may accordingly contribute to the development of severe complications during systemic infection (105). IL-6 is a proinflammatory cytokine synthesized by the skeletal muscle. The increased levels of plasma IL-6 has been reported in lipopolysaccharide induced human endotoxemia (93).

Kinase activity

Adenylate kinase 1 (AK1) is involved in muscle energetic economy and metabolic stress tolerance (57). Striated muscle preferentially expressed protein kinase (SPEG) gene, a sensitive marker for skeletal muscle differentiation (53). Mitogen-activated protein kinase-activated protein kinase 2 (MAPKAPK2) and mitogen-activated protein kinase kinase kinase 14 (MAP3K14) are required for skeletal muscle differentiation (18, 109) and these were also involved in the skeletal muscle atrophy through MAPK signaling via its downstream effectors like Gadd45 and p21 (26).

Protein metabolism

Atrogin-1, also known as MAFbx a member of SCF (SKP1-CUL-F-box protein) subfamily of E3 ligases and its mRNA levels increases during most muscle wasting conditions (11, 42). Different proteasome subunit complexes PSMD2, PSMD3 and PSMD11 cleave peptides in an ATP/ubiquitin-dependent process. The lysosomal cysteine proteinases (cathepsins CTSL, CTSL2 and CTSD) play an important role in intracellular protein breakdown. Metalloproteinase inhibitor 2 precursor (Timp2), endogenous Timp proteins are inhibitors of matrix metalloproteinase (Mmp) that act primarily by their ability to chelate Zn^{2+} and the inactive form of Mmp is stabilized by Timp2 thereby inhibiting the formation of the active proteolytic form of the

enzyme (19). These MMPs are involved in both extracellular and intracellular protein degradation (4).

Chemokine activity

Various chemokine genes were altered such as chemokine ligand 2 (CCL 2) or MCP-1, involved in sepsis induced muscle dysfunction (62). Chemokine receptor 7 (CXCR7) is involved in myogenic differentiation (95). CCL 19 and CCL 21 are the ligands for chemokine receptor 7 (CCR 7) and an increased expression of these ligands have been shown in muscles of polymyositis (139).

The deregulation of skeletal muscle contraction and/or muscle mass can lead to various muscle wasting diseases such as acute quadriplegic myopathy in intensive care unit patients.

Acute Quadriplegic Myopathy

Primary muscle involvement in ICU patients initially remained under recognized, but there has been great interest in multi model investigations of ICU paralysis syndromes, which have shown that AQM may be the most common, acquired neuromuscular disorder in ICU patients. A common and serious complication in ICU patients with critical illness is severe muscle weakness in combination with respiratory failure (45). A myopathy associated with critical illness was initially reported in a patient treated for status asthmaticus (84). This specific condition has been given more than ten different names besides AQM, such as, critical illness myopathy, thick filament myosin myopathy, acute myopathy in severe asthma, myopathy of intensive care etc (64). Specific for this type of myopathy is the apparent preferential loss of thick filament proteins; several triggering factors have been suggested to induce this condition, such as NMBA, CS and sepsis (64, 69, 119).

Acute muscle wasting and persistent weakness, mostly effecting limb muscles, are distinctive features of ICU patients with AQM (64). For many years AQM was considered to be a rare and of limited clinical significance due to miss or under diagnosis. AQM prevalence rate is not clear; some studies have revealed that it can vary between 35-42% in the ICU population (63).

AQM not only causes the significant muscle weakness, but can also lead to an increased ICU stay, higher morbidity rate and impaired rehabilitation. Additionally, the median hospital costs for AQM patients are $91,476 i.e., in excess of $66,713 as compared to ICU control patients (116). To treat the AQM patients, the cost increased to $2232-$4174 per day (125). The increased cost is partly due to the fact that the standard weaning time of the

patient from the ventilator is doubled in critically ill patients developing severe weakness, compared to those without (23).

Diagnosis

AQM is under diagnosed primarily due to insufficient diagnostic methods. The prevalence of AQM is not known, one-third of the ICU patients treated for status asthmaticus develops AQM (29). AQM is a primary myopathy with distinctive clinical, electrophysiological and morphological findings such as 1. The patient is critically ill (multiorgan dysfunction and failure), 2. Limb weakness or difficulty in weaning of patient from the ventilator, 3. Compound muscle action potential (CMAP) amplitudes less than 80% of the lower limit of normal in two or more nerves, 4. Sensory nerve action potential amplitudes more than 80% of the lower limit of normal, 5. Needle electromyography with short duration, low-amplitude motor unit potentials with early or normal full recruitment, with or without fibrillation potentials in conscious and collaborative patients; or increased CMAP duration or reduced muscle membrane excitability on direct muscle stimulation in non-collaborative patients, 6. Absence of a decremental response on repetitive nerve stimulation and 7. Muscle histopathological findings of primary myopathy (myosin loss or muscle necrosis) (64, 73). Serum creatine kinase (CK) elevation has been reported in some patients during the first week and it can serve as an additional diagnostic feature (29).

Even though the correct diagnosis of AQM is difficult for several reasons, such as the cooperation from patients required for EMG, many ICU patients are incapable of voluntary muscle contraction due to severe muscle weakness, deep sedation, neuromuscular blockade or encephalopathy (13). The differentiation between polyneuropathy and myopathy is complex by conventional EMG, leaving room for miss-diagnosis of AQM (76).The diagnosis of AQM is further complicated by several independent factors like primary disease, different pharmacological interventions, muscle biopsies taken several weeks after ICU admission and exposure to different causative agents.

Although it is an invasive procedure, a muscle biopsy is required for histological confirmation of AQM (34, 150). Electrophoretic separation of intracellular proteins from a muscle biopsy can reveal a selective loss of myosin and myosin associated proteins (a pathognomonic factor of AQM) (69, 71, 89). Muscle biopsy histopathology shows muscle fiber atrophy with preferential loss of type II fibers, fiber necrosis and regeneration. Furthermore extensive myosin loss can be observed in muscle biopsy cross sections using various methods such as electron microscopy, enzyme and immune cytochemical analysis of and gel electrophoresis. In all these techniques, electrophoretic separation of myofibrillar proteins by SDS-PAGE and myo-

sin to actin ratio has been suggested as superior, sensitive and rapid methods to diagnose AQM (71) (figure 7).

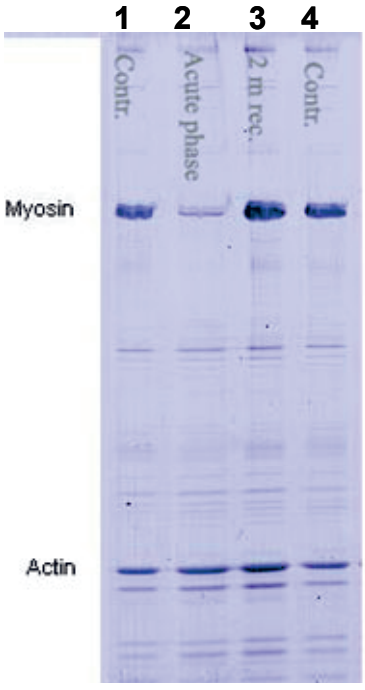

Figure 7. The 6% SDS-PAGE for AQM diagnosis. Lane's 1and 4 represent controls, lane 2 represents acute phase of the disease (decreased myosin to actin ratio) and full recovery after 2 months in lane 3.

Interventions and risk factors

Many ICU patients who are exposed to numerous intervention strategies, they are typically mechanical ventilated receive analgesia and are sedated during hospitalization. The principle aims of these interventions are to provide comfort and minimize pain, suffering, anxiety, and other forms of distress to the patient, some of which are the result of ICU interventions. However the dose and time of different interventions in the ICU can in fact cause the muscle wasting and loss of muscle function observed in the patients.

The following interventions are mostly used in the ICU which will cause the AQM.

Mechanical ventilation

Mechanical ventilation is required when the body cannot meet its oxygen demand through spontaneous breathing or when the body cannot adequately remove carbon dioxide (CO_2). Different conditions can increase the oxygen demand, such as abnormalities in the respiratory system, neuromuscular disease, or cardiovascular system failure. Critically ill patients who are admitted to the ICU typically require mechanical ventilation (MV) and are immobilized for long time periods. Muscle specific differences and the time period of immobilization also play a major role in the severity of the muscle atrophy.

Neuromuscular blocking agents (NMBA)

NMBA have been forwarded as a factor triggering AQM in ICU patients. However the generalized muscle weakness of AQM should be differentiated from the prolonged paralysis associated with the discontinuation of NMBA. It has been shown that there is a positive correlation reported between the dose and duration of NMBA therapy and the possibility of developing a myopathy (29). NMBA are metabolized by the liver and cleared by the kidney. Extended the effect of NMBA may accordingly have prolonged effects that may persist for several days after the use of the drug has been discontinued (124).

It has been suggested that NMBA such as pancuronium bromide, a biquaternary amino steroid, or the shorter acting vecuronium, and steroids, singly or in combination trigger the primary myopathy. These compounds are generally used for more than 24 hours, but occasionally for days and weeks. When they are discontinued, complexity in weaning from the ventilator and limb paralysis are prominent.

Corticosteroids

Different experimental studies reveal deleterious effects of corticosteroids on the neuromuscular system. A prospective study showed that corticosteroids are the key factors triggering muscle weakness in ICU patients (24). Furthermore rats receiving corticosteroids have shown structural muscle changes that are similar to those that are observed in critically ill patients (88, 115). Patients who get more than 5mg of hydrocortisone were reported to develop a myopathy (131). Some steroids such as the fluorinated corticosteroids trimicinolone, tamethasone, and dexamethasone are involved in muscle weakness. Actually, dexamethasone has been found to promote enhanced protein breakdown and increased expression of the genes generally involved in the ubiquitin-proteasome proteolytic pathway (39). Corticosteroids can also induce several different transcriptional factors activating various proteolytic pathway genes leading to muscle fiber atrophy (3, 43, 120). Not only is the muscle degradation but protein synthesis is also impaired as evidenced by the up-regulation of 4EBP1 (129).

Sepsis

Sepsis is a leading cause of death in intensive care unit patients. Sepsis is characterized by a body temperature of 39^0C or more or below 35.5^0C, a heart rate of 90 beats per minute or more, a respiratory rate of more than 10 liters per minute, and a known or strongly suspected infection (22). There is ample scientific indication that sepsis induces a myopathy characterized by reductions in the force-generating capacity and atrophy (138). Mitochondrial dysfunction has been shown to be correlated with septic shock (14). Proinfammatory cytokines (TNFα and IL-6) and chemokine activity (MCP-1) genes have been reported to be involved in the reduction of force-generating capacity of the contractile proteins (62). Muscle wasting occurs later in the course of systemic inflammation and results in increased proteolytic degradation and decreased protein synthesis. The ubiquitin ligases atrogin-1 and MuRF1are important players in the sepsis induced muscle atrophy (42, 74).

Muscle disparities

The process of muscle wasting differs between the diverse groups due to their embryonic origin, muscle fiber constitution and post-natal development of the muscle. In ICU patients, diaphragm muscle dysfunction occurs within hours of the initiation of the MV (80). Limb muscles are typically severely affected at a later stage, i.e., after several days of ICU treatment, and craniofacial muscles are less or not affected.

Craniofacial muscle

The head muscles originate from cranial mesoderm (101). Branchiomeric muscles that are involved in mastication, facial expression, function of the larynx and pharynx are derived from pharyngeal mesoderm, which includes both lateral splanchnic and paraxial mesoderm (78).

However a disparity exit between head and trunk muscles as they have different gene regulatory programs, for instance, *pax3* is an important upstream regulator of trunk myogenesis (15), but it is not expressed in head mesoderm. *Tbx1* and *Pitx2* genes , on the other hand, are upstream regulators of skeletal myogenesis in the head, but not in the trunk (46).

In the post-natal period, fiber type differences continue, where the adult craniofacial muscle fibers maintain fetal myosin heavy chain (MyHC) isoform expression and in some species α-cardiac MyHC (146, 148). Masticatory muscle fibers are different in several characteristics from limb muscle fibers, such as smaller CSA and type II fibers being smaller than type I (32). During ageing, several limb muscles exhibit a fast to slow shift in fiber type proportions, while a slow to fast fiber type shift has been observed in the masseter muscle (98).

Limb muscle

In mammals, skeletal muscles are still immature at birth and important changes in the fiber type takes place during early stages of the postnatal development. The postnatal changes in the fiber type profile can be explained by the collective action of an intrinsic genetic program and of extrinsic factors, such as hormonal and neural influences, acting on the myonuclei of the myofibers themselves. On the other hand, the possibility of developmental changes of satellite cells incorporated into the growing myofibers of neonatal muscle also need to be considered (121). Direct evidence for satellite cell transformation was recently reported with respect to the role of the transcription factor Pax7. The *Pax7* gene was inactivated at different developmental periods using an inducible knockout approach (77).

Biceps femoris is a posterior thigh muscle and it belongs to the hamstring muscle group. The embryonic origin of biceps femoris muscle is from mesenchyme of the limb buds. 1/4 th of the fibers are slow-twitch and 3/4 th of the fibers are fast-twitch (44). The fiber type profile of skeletal muscles undergoes important changes during subsequent stages in postnatal life and aging.

Diaphragm muscle

The diaphragm is the main inspiratory muscle. It works continuously and generally at a low intensity. From a general point of view, functional and biochemical characteristics of the diaphragm is similar to those of other skeletal muscles with a similar fiber type composition. However, fibers expressing slow- and fast-twitch MyHC isoforms are present in equal proportions in the adult human diaphragm. A small fiber size, abundance of capillaries, and a high aerobic oxidative enzyme activity are typical features of diaphragm fibers, i.e., in accordance with a high fatigue resistance required for continuous respiratory activity (108).

It is made clear that many different primary diseases, large variability in pharmacologic treatment, collection of muscle samples several weeks after admission to the ICU, and exposure to different causative agents are all factors complicating mechanistic studies of muscle paralysis and wasting in the clinical ICU setting. Thus there is, accordingly, a compelling need for animal models mimicking ICU conditions (66). In an attempt to unravel these muscle specific differences in the response to the ICU intervention alone and/or in combination with sepsis or corticosteroids, gene expression analyses and single muscle fiber contractile measurements have been conducted in masticatory, limb and diaphragm muscle using a unique porcine ICU model.

Aims of the present investigation

General aim

The general goal of this study was to gain knowledge regarding the gene expression, protein degradation and muscle specific differences in response to the ICU condition. In accordance with the stated objective, a porcine ICU model was used to address the muscle specific gene expression in response to MV, NMBA, sepsis and CS separately or in combination.

Specific aims

1. Identify gene expression changes underlying the sparing of masticatory versus limb muscles in the experimental pig ICU model (Paper I).
2. Determine the role of sepsis on gene expression in limb muscles (Paper II).
3. Determine the effects of corticosteroids on gene expression in limb muscles (Paper III).
4. Explore the mechanisms underlying diaphragm muscle weakness in the pig ICU model (Paper IV).

Materials and Methods

Animals (Paper I, II, III and IV)

A total of 18 female domestic piglets (23–30 kg body weight) were included. All piglets originated from the same farm (Vallrums Lantbruk, Ransta, Sweden) and were kept in 12 square meter pens with hay, straw, and wood shavings as bedding material. They were housed at 18–19°C and relative humidity of 45–55% under natural day-night rhythm with liberal access to feed (Smagrisfoder Solo 331; Lantmannen, Stockholm, Sweden), water, and environmental enrichment. Food, but not water, was withheld for 12 h before induction of anesthesia. The Ethical Committee on Animal Research at the Karolinska Institute, Stockholm, Sweden, approved the study protocol (Dnr N71/98, N54/02 and N75/04).

Intervention (Paper I, II, III and IV)

The pigs were sedated with medetomidine (Dormitor vet 1mg/ml, Orion Pharma AB, Stockholm, Sweden) and zolazepam (Zoletil 250, Reading, Carros, France) before an intravenous access was placed, and 100mg of ketamine (Ketaminol vet 50mg/ml, Intervet, Boxneer, Netherlands) was administered. Following tracheostomy, all animals were mechanically ventilated using volume-controlled ventilation (Siemens 900A ventilator; Siemens Elema, Solna, Sweden) adjusted to an initial FiO_2 of 0.21–0.30, an inspired tidal volume of 10 $ml \cdot kg^{-1}$and a respiratory rate of 20 breaths per min, with an I:E ratio of 1:2 and inspiratory rise time of 5-10%. During the remaining study period, the settings were adjusted carefully to maintain arterial oxygen and carbon dioxide tensions within normal limits and to avoid high airway pressures and risk of barotrauma. Sedation was titrated to promote immobilization and allow ventilator synchrony by inhibiting spontaneous breathing activity. Anesthesia was maintained and adjusted through a novel anesthetic conserving device (AnaConda, Sedana Medical, Sundbyberg, Sweden) which permits administration of an inhaled anesthetics via a syringe pump to the inspired gas mixture, as previously described (117). During this study period, isoflurane (Abbott Laboratories, Chicago, Il, USA) was delivered at 0.8 – 1.3% end-tidal concentration and supplemented by intravenous bolus doses of morphine and ketamine as needed to provide immobilization. Core body temperature (blood) was maintained in the range of 38.5 – 40°C by a servo controlled heating pad. Animals received 2000 – 4000 ml/day as a continuous intravenous infusion of a crystalloid solution

(Ringeracetat, Fresenius Kabi, Stockholm, Sweden) to maintain stable blood pressure and urinary output throughout the experimental period and an intravenous glucose infusion (Rehydrex, Fresenius Kabi, Stockholm, Sweden, 25 mg glucose /mL) at 1 – 1.5 ml/kg/hr titrated to maintain blood glucose between 4-8 mmol/L to decrease the effects of catabolism. In addition, each animal received prophylactic streptomycin 750 mg/d and bensylpenicillin 600 mg/d (Streptocillin Vet, Boeringer-Ingelheim, Hellerup, Denmark). Arterial oxygen and carbon dioxide tensions, acid-base balance, electrolytes and blood glucose levels were monitored regularly and kept within normal range throughout the study period. A neuromuscular blocking agent (NMBA) was administered as a continuous infusion of rocuronium (Esmeron, Organon, Boxtel, The Netherlands) 25 mg/hr for 5 days while a corticosteroid (CS) was given as bolus doses of hydrocortisone (Solu-Cortef, Pfizer AB) 50 mg three times daily for 5 days. Endotoxemia was induced after completion of the surgical preparation on day 1 by administration of a continuous infusion of *Escherichia coli* endotoxin, serotype O26:B6 (Sigma Chemical, St.Louis, Missouri, USA) at a rate titrated to physiological effects (mean blood pressure decrease of >30% and a pulmonary artery occlusion pressure increase of 50%) with a mean total dose of 8 μg/kg.

Expression profiling (Paper I, II and III)

Three micrograms of total RNA from the muscle samples were extracted and processed to generate biotin-labeled cRNA as previously described (20). Each sample was then hybridized to Affymetrix Porcine Genome Array containing 23,937 probes representing 20,201 genes. Standard operating procedure and quality control was done as previously described (20). Muscle samples from the animals on day 1 and day 5 were profiled. All profiles have been made publicly accessible via National Centre for Biotechnology information Gene Expression Omnibus (GSE24239; GSE33037; GSE37166 http://www.ncbi.nlm.nih.gov/geo).

Microarray data normalization and analysis (Paper I, II and III)

Subsequent analysis of the gene expression data was carried out in the freely available statistical computing language R (http://www.r-project.org) using packages available from the Bioconductor project (www.bioconductor.org). The raw data was normalized using the robust multi-array average (56) background-adjusted, normalized and log-transformed summarized values first suggested by Li and Wong in 2001 (81). In order to search for the differentially expressed genes between the samples from the different days an empirical Bayes moderated t-test was applied (136), using the 'limma' package. A linear model was fitted to the data, Day5 *vs.* Day1 effects were estimated. To address the problem with multiple testing, the *p*-values were adjusted according to Benjamini and Hochberg. Significant probe sets with an adjusted *p*-value < 0.05 were selected for further investigation and more than a 2-fold change were included in further analyses. Since the porcine array is

minimally annotated and is not identified by web based analysis software, we used published putative human homologues (143). Up- and down-regulated transcripts were further analyzed and categorized using DAVID web based functional annotation tool (http://david.abcc.ncifcrf.gov/) (54). Some of the functional categories were combined and some categorization was done manually, to improve the interpretative value of the data. Clustering images were developed using Genesis software (137).

cDNA synthesis (Paper I, II, III and IV)

cDNA for all papers was prepared using qScript ™ cDNA SuperMix (Quanta Biosciences, Inc. MD 20877, USA) according to the instructions from the manufacturer.

Quantitative real time RT-PCR (Paper I, II, III and IV)

Reverse transcription and quantitative PCR analysis was performed as previously described (102). Briefly, total RNA (100ng) was reverse transcribed to cDNA using Qscript cDNA supermix (Quanta Biosciences, USA). cDNA was amplified in triplicate using MyiQ™single color real time PCR detection system (Bio-Rad Laboratories, Inc., Hercules, CA, USA), and used to quantify the mRNA levels for porcine Atrogin-1, HSP 110/105, FOXO1A, αB-crystallin, FOS, STAT3, MYOM2, IRS1, CEBPB, PGC1-β, myostatin, MAP1A, SOD2, MyHC I, MyHC IIx and 18S. The thermal cycling conditions include 95ºC for 9 minutes, followed by 50 cycles of amplification at 95ºC for 15 sec, followed by 60ºC for 1 minute. Each reaction was performed in a 25µl volume with 0.4µM of each primer and 0.2µM probe or SYBR green (1988123, Roche Diagnostics, GmBH, Ulm, Germany). Taq man primers and probes were designed using Primer Express® program (Applied Bio System, Foster City, CA, USA). Porcine 18S gene was used as the internal control. Primer sequences for porcine Atrogin-1 and HSP 105/110 were published elsewhere (8, 102, 106).

Total protein quantification (Paper I, II, III and IV)

To quantify the total protein, cryosections of muscle biopsy were obtained and submerged in to 8M urea buffer, with subsequent centrifugation and sonication. This sample was then used for total protein quantification using the NanoOrange® Protein Quantification Kit (Molecular Probes, Inc., Eugene, OR, USA). The fluorescence of the samples was measured using a Plate Chameleon™ Multilabel Platereader (Hidex Oy, Finland) and related to a standard curve. Values were obtained by using the software MikroWin, version 4.33 (Microtek Laborsysteme GmbH, Overath, Germany).

Immunoblotting (Paper I, II, III and IV)

SDS-PAGE was performed by using Mini-PROTEAN® 3 Cell (Bio-Rad Laboratories, 2000 Alfred Nobel drive, Hercules, CA, USA). Five µg of total

protein were used. Electrophoresis was performed at 120 volts for 1hour 30mins; gels were subjected to polyvinylidene fluoride (PVDF) membranes (GE Healthcare) and transfer the blot for 1hour at 350mA current. Membranes were incubated with HSP 70 (SMC 100A/B, Stress Marq Biosciences Inc, BC, Canada), HSP 90 (AC88, Stressgen, Ann Arbor, MI), Apg 2 (sc-6240, Santa Cruz biotechnology Inc., CA, USA), SOD2 (ab13533, Cambridge Science Park, CB4 0FL, UK), FOXO1A (sc-11350, Santa Cruz Biotechnology Inc., CA, USA), Atrogin-1 (AP2041 ECM Biosciences, KY, USA), αB-crystallin (SMC 159A/B, Stress Marq Biosciences Inc, BC, Canada), p62 (P0067, Sigma-Aldrich, MO, USA), UNC45B (a generous gift by Brian Stanley/Jennifer Van Eyks lab) and Actin (sc-1616, Santa Cruz Biotechnology Inc., CA, USA) primary antibodies. Protein detection was performed by incubating the membranes with secondary antibodies NA931 or NA934 (GE Healthcare) and using ECL Advance western blotting detection kit (RPN 2135, GE Healthcare) according to the manufacturer's instructions. Of all signal intensities were normalized to Actin signal intensity, followed by scanning the gels (Molecular Dynamics) and measuring the intensity volume (Image Quant TLv 2003, Amersham Biosciences).

Statistical analysis (Paper I, II, III and IV)

For the single muscle fiber size and function, Sigma Stat software (Jandel Scientific) was used to generate descriptive statistics. Given the small number of pure type IIb and hybrid type I/IIa and IIx/IIb fibers observed in the single muscle fiber experiments, comparisons were restricted to muscle fibers expressing the type I, IIa, IIa/IIx and IIx MyHC isoforms. A two-way ANOVA (day x fiber type) was performed followed by the Tukey's test (level of significance $P<0.05$). Values are means and standard error of means (SE). *T-test* was used to test statistical significance for both the quantitative RT-PCR and western blotting experiments.

Muscle biopsies (Paper I, II, III and IV)

Muscle biopsies of the masseter and biceps femoris were obtained from animals on two separate occasions, i.e., on day 1 before administration of NMBA, CS and endotoxin (control biopsy) and on day 5 (after intervention). The biopsy on day 1 was taken from both the left or right masseter and biceps femoris muscle while the biopsy on day 5 was taken from the contralateral side, in order to eliminate the risk of interference induced by the biopsy procedure. Biopsies were split in two portions; one part was frozen in liquid propane cooled by liquid nitrogen and stored at -80°C for later analysis while the other part was immediately placed in an ice-cold relaxing solution (in mmol/l: 100 KCl, 20 Imidazole, 7 $MgCl_2$, 2 EGTA, 4 ATP, pH 7.0; 4°C). Small bundles of ~25-50 fibers were dissected free from the muscle and tied to a glass micro capillary tube at ~110% resting length. The bundles were then placed in a skinning solution (relaxing solution containing glycerol; 50:50 v/v) at 4°C for 24 h and subsequently stored at -20°C for use with-

in 3 weeks, or treated with a cryoprotectant (sucrose solution) for long-term storage at -80°C as described earlier (38).

Single muscle fiber experimental procedure (Paper I and IV)

On the day of an experiment, a fiber segment 1 to 2 mm long was left exposed to the experimental solution between connectors leading to a force transducer (model 400A, Aurora Scientific) and a lever arm system (model 308B, Aurora Scientific) (99). The apparatus was mounted on the stage of an inverted microscope (model IX70; Olympus). While the fiber segments were in relaxing solution, the sarcomere length was set to 2.65-2.75 μm by adjusting the overall segment length (70).The diameter of the fiber segment between the connectors was measured through the microscope at a magnification of ×320 with an image analysis system prior to the mechanical experiments. Fiber depth was measured by recording the vertical displacement of the microscope nosepiece while focusing on the top and bottom surfaces of the fiber. The focusing control of the microscope was used as a micrometer. Fiber cross-sectional area (CSA) was calculated from the diameter and depth, assuming an elliptical circumference, and was corrected for the 20% swelling that is known to occur during skinning (99).

Relaxing and activating solutions contained (in mM) 4 Mg-ATP, 1 free Mg^{2+}, 20 imidazole, 7 EGTA, 14.5 creatine phosphate, and KCl to adjust the ionic strength to 180 mM. The pH was adjusted to 7.0. The concentrations of free Ca^{2+} were 10^{-9} M (relaxing solution) and $10^{-6.2}$, $10^{-6.0}$, $10^{-5.8}$, $10^{-5.5}$, $10^{-5.2}$, $10^{-4.9}$ and $10^{-4.5}$ M (activating solutions), expressed as pCas (i.e., -log [Ca^{2+}]). Apparent stability constants for Ca^{2+}-EGTA were corrected for temperature (15 ^{0}C) and ionic strength (180 mM). The computer program of Fabiato (33) was used to calculate the concentrations of each metal, ligand, and metal-ligand complex.

At 15 ^{0}C, immediately preceding each activation, the fiber was immersed for 10-20 s in a solution with a reduced Ca^{2+}-EGTA buffering capacity. This solution is identical to the relaxing solution except that the EGTA concentration is reduced to 0.5 mM, which results in more rapid attainment of steady-state force during subsequent activation. Maximum velocity of unloaded shortening (V_0) was measured by the slack-test procedure (31). Fibers were activated at pCa 4.5 and once steady tension was reached, various amplitudes of slack (ΔL) were rapidly introduced (within 1-2 ms) at one end of the fiber. The time (Δt) required to take up the imposed slack was measured from the onset of the length step to the beginning of tension redevelopment. For each amplitude of ΔL, the fiber was re-extended while relaxed in order to minimize non-uniformity of sarcomere length. A straight line was fitted to a plot of ΔL vs Δt, using a least-squares regression, and the slope of the line was recorded as V_0 for that fiber. Maximum active tension (P_0) was calculated as the difference between the total tension in the activating solution (pCa 4.5) and the resting tension measured in the same segment while in the

relaxing solution. All contractile measurements were carried out at 15 ^{0}C. The contractile recordings were accepted in subsequent analyses if a V_0 value was based on linear regressions including four or more data points, and data were discarded if *r* for the fitted line was less than 0.97, if SL during isometric tension development changed by more than 0.10 μm compared with SL while the fiber was relaxed or if force changed more than 10% from first to final activation (99). Specific tension (ST) was calculated as maximum tension (P_0) normalized to CSA.

Stiffness. Once steady-state isometric force was reached, small-amplitude sinusoidal changes in length (ΔL: ± 0.2% of fiber length), were applied at 500 Hz at one end of the fiber (86). The resultant force response (ΔF) was measured, and the mean of 20 consecutive readings of ΔL and ΔF was used to determine stiffness. The actual elastic modulus (E) was calculated as the difference between E in activating solutions and resting E measured in the same segment in the relaxing solution. E was determined as follows (92).

$$E = (\Delta F/\Delta L) \times (\text{fiber length/CSA})$$

Relative force-pCa and stiffness-pCa relationships. Each fiber was exposed to different solutions with varying pCas (pCa 9.0–4.5). Force and stiffness were normalized to maximum force and stiffness at pCa 4.5 allowing the construction of relative force-pCa and relative stiffness-pCa curves. To determine the midpoint (termed pCa_{50}) and the Hill coefficient (*n*H) from the pCa curves, data were fitted (SigmaPlot 5.0 and Origin 6.1 Professional software; Jandel Scientific) using the Hill equation in the following form:

$$X = 100 \times [Ca^{2+}]^{nH} / ([Ca_{50}]^{nH} + [Ca^{2+}]^{nH})$$

X is the relative force or relative stiffness. -log $[Ca_{50}]$ is the midpoint (pCa_{50}). *n*H is the Hill coefficient.

After the mechanical measurements, each fiber was placed in urea buffer (120 g urea, 38 g thiourea, 70 ml H_20, 25 g mixed bed resin, 2.89 g dithiothreitol, 1.51 g Trizma base, 7.5 g SDS, 0.004 % bromophenol blue) in a plastic micro centrifuge tube and stored at -80 ^{0}C for subsequent electrophoretic analyses.

Measurement of reactive carbonyl derivatives (Paper IV)

The reactive carbonyl derivatives of myosin and actin were determined using the Oxy-Blot protein oxidation detection kit (Invitrogen) via 12% SDS-PAGE gels and Western blotting (149). All the samples were loaded with identical volumes and protein quantities (2.5 μg each). The reactive carbonyl derivatives were quantified using a soft laser densitometer (arbitrary unit).

Sodium Dodecyl Sulphate -Polyacrylamide gel electrophoresis (SDS-PAGE) (Paper I and IV)

The myosin heavy chain (MyHC) composition was determined by 6% SDS-PAGE. The total acrylamide and bis concentrations were 4% (w/v) in the stacking gel and 6% in the running gel, and the gel matrix included 30% glycerol. The ammonium persulphate concentrations were 0.04% and 0.029% in the stacking and separation gels, respectively, and the gel solutions were degassed (<100 millitorr) for 15 min at 18 ^{0}C. Polymerisation was subsequently activated by adding TEMED to the stacking (0.1%) and separation gels (0.07%). Sample loads were kept small to improve the resolution of the MyHC bands and electrophoresis was performed at 120 V for 22-24 h with a Tris-glycine electrode buffer (pH 8.3) at 15 ^{0}C (SE 600 vertical slab gel unit, Hoefer Scientific Instruments, USA, for details see(68, 70).

Total MyHC and actin content (Paper I and IV)

Myosin and actin quantification was determined by 12% SDS-PAGE. The acrylamide concentration was 4% (w/v) in the stacking gel and 12% in the running gel, and the gel matrix included 10% glycerol. Volumes of 5 µl of the samples were loaded together with 5 µl of the standard dilutions. The standard was prepared by pooling sections from control rats' EDL and soleus muscles. The myofibrillar protein standards were prepared, assuming that actin and myosin contents were 12.5 and 25% of the total protein content, respectively. Linear actin and myosin curves were observed within the 5-200 µg/ml range, but the calibration curves were not parallel. Electrophoresis was performed at 32.0 mA for 5 h with a Tris-glycine electrode buffer (pH 8.3) at 15 ^{0}C (SE 600 vertical slab gel unit; Hoefer Scientific Instruments). The gels were stained using *SimplyBlue™ SafeStain (Invitrogen)* and subsequently scanned in a soft laser densitometer (Molecular Dynamics, Sunnyvale, CA, USA) with a high spatial resolution (50 µm pixel spacing) and 4096 optical density levels. The volume integration function was used to quantify the amount of protein on 12% and 6% gels (ImageQuant TL Software v. version 3.3, Amersham Biosciences, Uppsala, Sweden).

Results and Discussion

Are there any differences in the gene expression of masticatory versus limb muscle function in an experimental critical illness model? (Paper I)

A unique porcine ICU model was used in this study. In this model, pigs were immobilized, mechanically ventilated, sedated and exposed to the factors triggering AQM, i.e., NMBA, CS and sepsis for five days. Both single fiber CSA and specific force (P_0/CSA) were preserved during the five-day experimental period in fibers expressing type I, IIa, IIa/IIx and IIx MyHC isoforms in the masseter muscle of piglets exposed to the ICU intervention. These results are in sharp contrast to our previous results in limb (biceps femoris) muscle fibers, showing a dramatic decline ($p<0.05$) in specific force (Fig. 8.). Analyses of gene expression profile and validation demonstrate that, during the interventions and time period described above, there was a significant differential expression in a number of functional gene clusters.

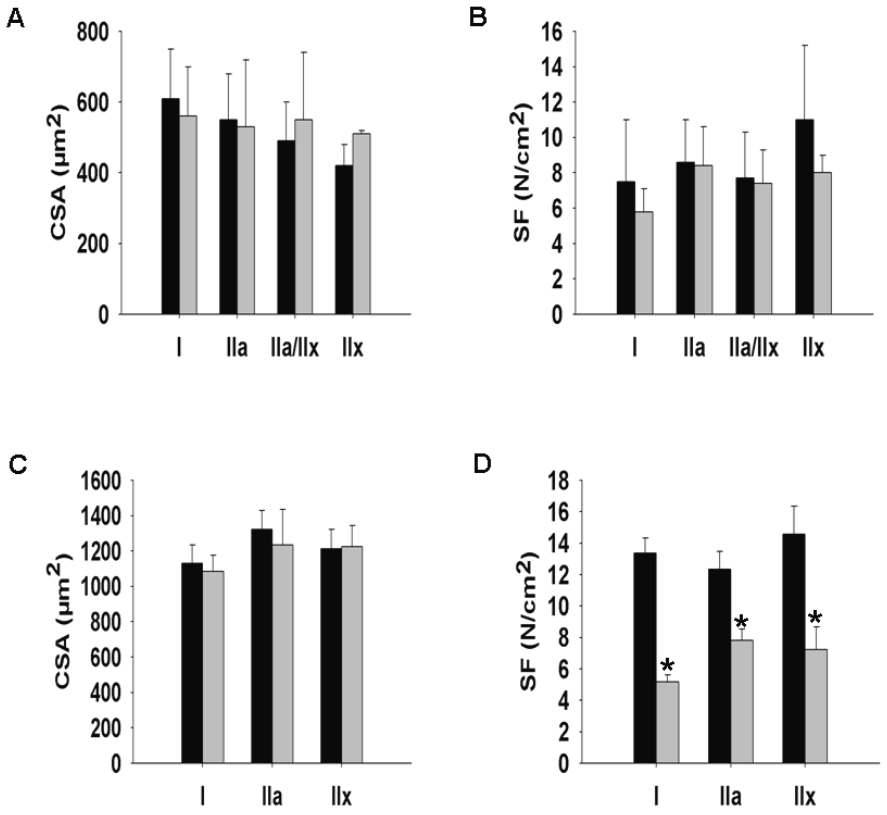

Figure 8. The masseter and biceps femoris single muscle fiber cross-sectional area (CSA) and specific force (SF, P_0/CSA). A: CSA of masseter type I, IIa, IIa/IIx and IIx muscle fibers on day 1 (black bars) and day 5 (gray bars); B: Specific force of masseter type I, IIa, IIa/IIx and IIx muscle fibers on day 1 (black bars) and day 5 (gray bars); C: CSA of biceps femoris type I, IIa and IIx muscle fibers on day 1 (black bars) and day 5 (gray bars); D: Specific force of biceps femoris type I, IIa and IIx muscle fibers on day 1 (black bars) and day 5 (gray bars). [C]and [D] were obtained from (Ochala et al 2011, PLoS ONE 6: e20876). Values are means + S.E.M.

The masseter up-regulated gene clusters includes transcription/growth factors, protein degradation, heat shock proteins, GTP binding, cell cycle, oxidative stress responsive, mitochondrial/energy and immune response. Limb muscle (biceps femoris) gene expression analysis reveals the up-regulated gene clusters including WD repeat containing, proteasome subunit, cell cycle regulation, protein synthesis, heat shock proteins, co-chaperone and transcriptional regulation.

The masseter down-regulated gene clusters include transcription/growth factors, muscle protein, mitochondrial, carbohydrate metabolism, G-protein and related and protein modification. Limb muscle (biceps femoris) gene expression analysis reveals the down-regulated gene clusters including mitochondrial, extracellular matrix, sarcomeric protein, ATP synthase, ankyrin, EGF-like domain containing, glycogen related and IGF-binding. In the masseter muscle in accordance with microarray data, real-time RT-PCR results indicated an up-regulation of the following genes: Atrogin-1 (3.31-fold), αB-crystallin (3.07-fold), HSP 110 (3.97-fold) and FOXO1A (2.61-fold). Down-regulation was confirmed in: myostatin (-5.16-fold) and PGC1-β (-1.96-fold) (figure 9.)

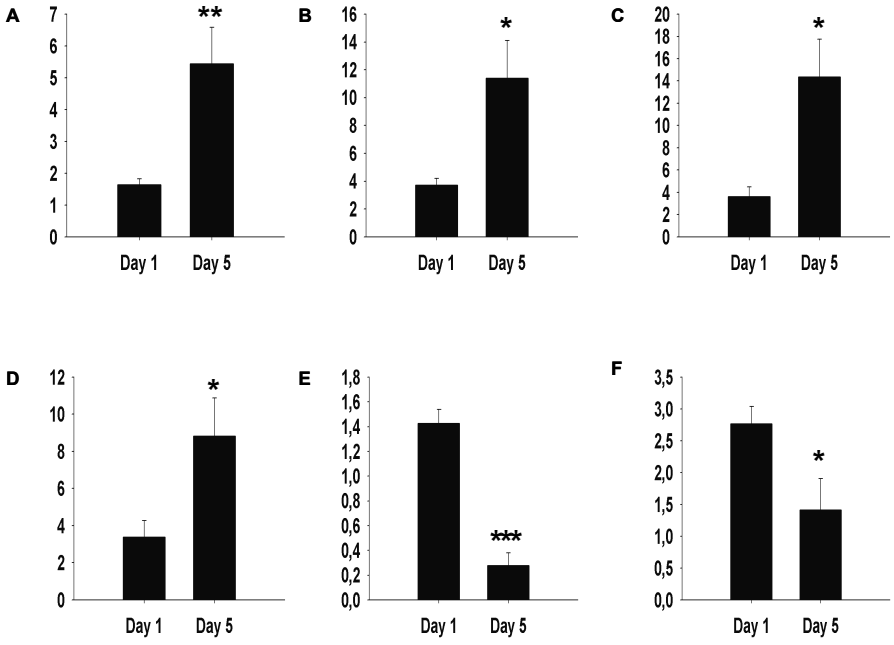

Figure 9. Microarray results were validated by real time RT-PCR in the masseter muscle. Atrogin-1 (A), αB- crystallin (B), HSP 105/110 (C) and FOXO1A (D) were up-regulated, while Myostatin (E) and PGC1-β (F) were down-regulated. Statistically significant differences versus the control group are denoted * ($p < 0.05$), ** ($p < 0.01$), and *** ($p < 0.001$).

At the protein level, a significant increase was observed in the following proteins: HSP 70 (2-fold), αB-crystallin (1.4-fold), P62 (5.8-fold) and SOD2 (1.4-fold). Further, a trend towards an increase was observed in the following proteins: HSP 90, APG 2 and Atrogin-1. FOXO1A did not show a detectable change in response to the ICU intervention (figure 10).

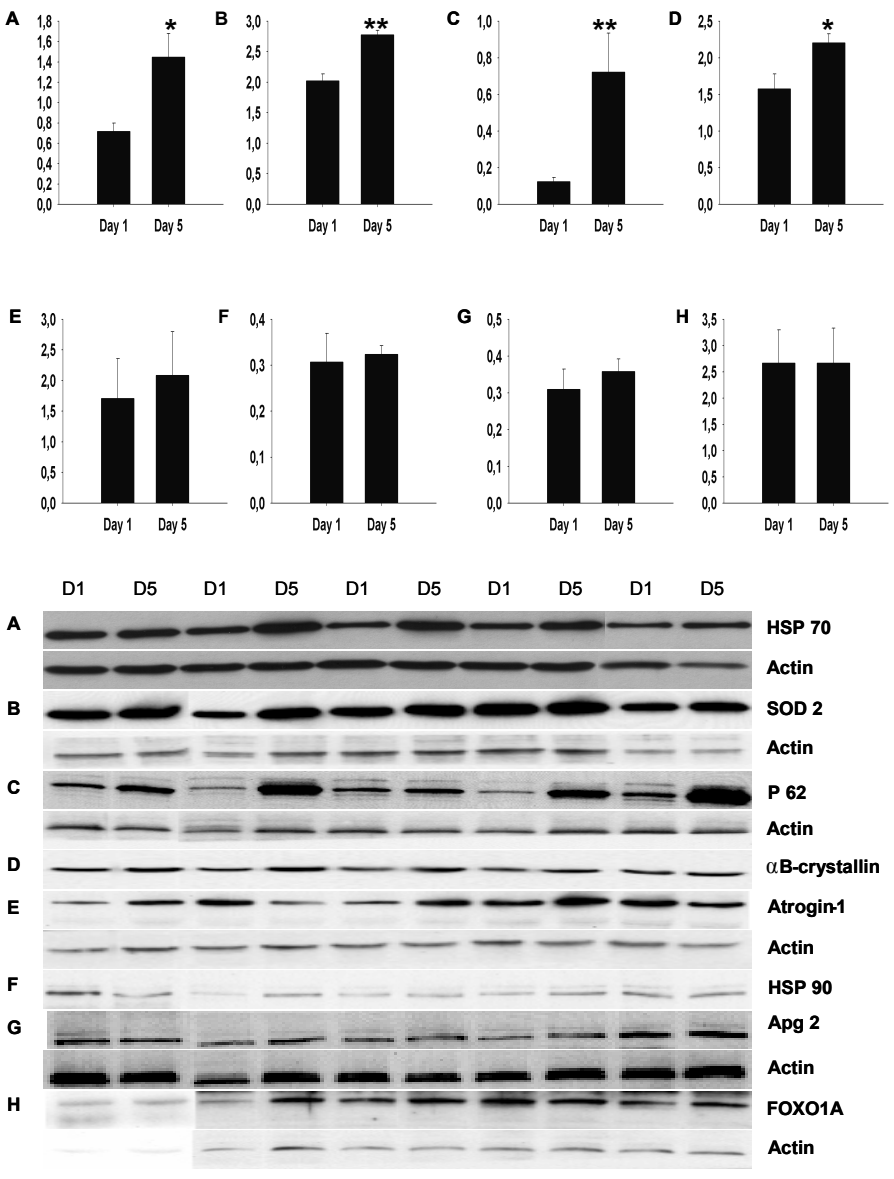

Figure 10. Western blot analyses in the masseter muscle for the following proteins: HSP70 (A), SOD2 (B), p62 (C), αB-crystallin (D), Atrogin-1 (E), HSP 90 (F), Apg 2 (G), and FOXO1A (H), normalized to Actin contents. Values are means + S.E.M. Statistically significant differences are denoted * ($p < 0.05$) and ** ($p < 0.01$).

These results suggest severe oxidative stress, initiation of protein degradation concomitant with protein protection pathways such as elevation in a number of heat shock protein genes, oxidative stress responsive genes and the negative regulator of MMP2, i.e., TIMP 2. Single fiber analyses demonstrate a maintained fiber CSA and force generating capacity (specific force) in the masseter muscle in response to the ICU intervention. This is in sharp contrast to our observations in limb (biceps femoris) and respiratory muscles. Single fiber analyses demonstrate a maintained fiber CSA but force generating capacity (specific force) was significantly decreased after the five day period.

The negative regulator of skeletal muscle growth myostatin, a TGF-β super family member and a gene which is involved in mitochondrial biogenesis, PGC1β, were down-regulated. Gene expression and functional analysis of single muscle fibers suggested that the sparing of the masseter muscle in this condition is due to up-regulation of several heat shock protein genes and down-regulation of the myostatin gene (Paper I).

Will sepsis play a prominent role in the limb muscle dysfunction? (Paper II)

Gene profiling revealed significant differences in animals mechanically ventilated with or without endotoxin induced sepsis. The up-regulated gene clusters include chemokines, immune response, transcriptional binding/regulation, kinase activity, G-protein regulated, DNA binding, ion channel, zinc binding, nucleotide binding and EGF-like.

The down-regulated gene clusters include heat shock proteins, cell cycle regulation, protein metabolism, cytoskeletal & sarcomeric, oxidative stress responsive, RNA processing, protein phosphorylation, nuclear pore complex, transcriptional regulation, GTP-binding, ion channel, zinc finger related and integral membrane. In accordance with microarray data real time RT-PCR results demonstrate a general up-regulation of the following genes: FOS (A), STAT3 (B), MYOM2 (C), IRS1 (D) and CEBPB (E). Down-regulation was confirmed in: MAP1A (F) (-4 fold) and SOD2 (G) (-9 fold) (figure 11).

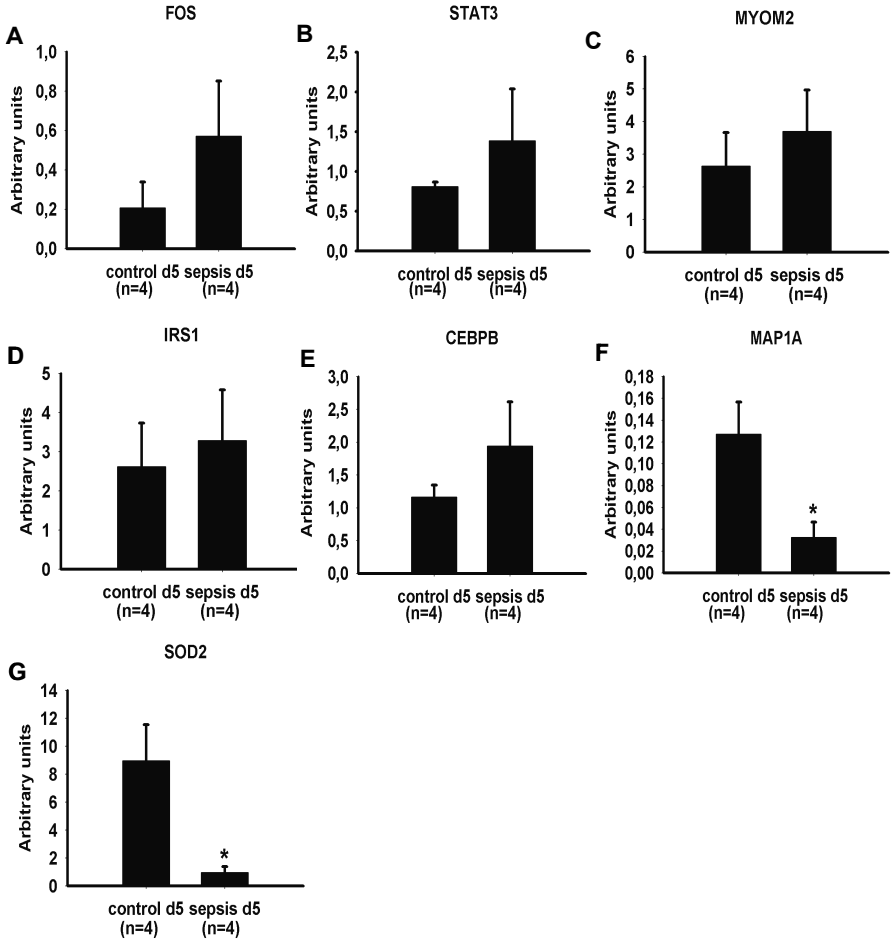

Figure 11. Microarray results were validated by real time RT-PCR in the biceps femoris muscle. FOS (A), STAT3 (B), MYOM2 (C), IRS1 (D) and CEBPB (E) were up-regulated, while MAP1A (F) and SOD2 (G) are down-regulated. Statistically significant differences versus the control group are denoted * ($p < 0.05$).

At the protein level, a general increase was observed in the UNC45B and a general decrease was observed in HSP70, αB-crystallin and SOD2 (figure 12).

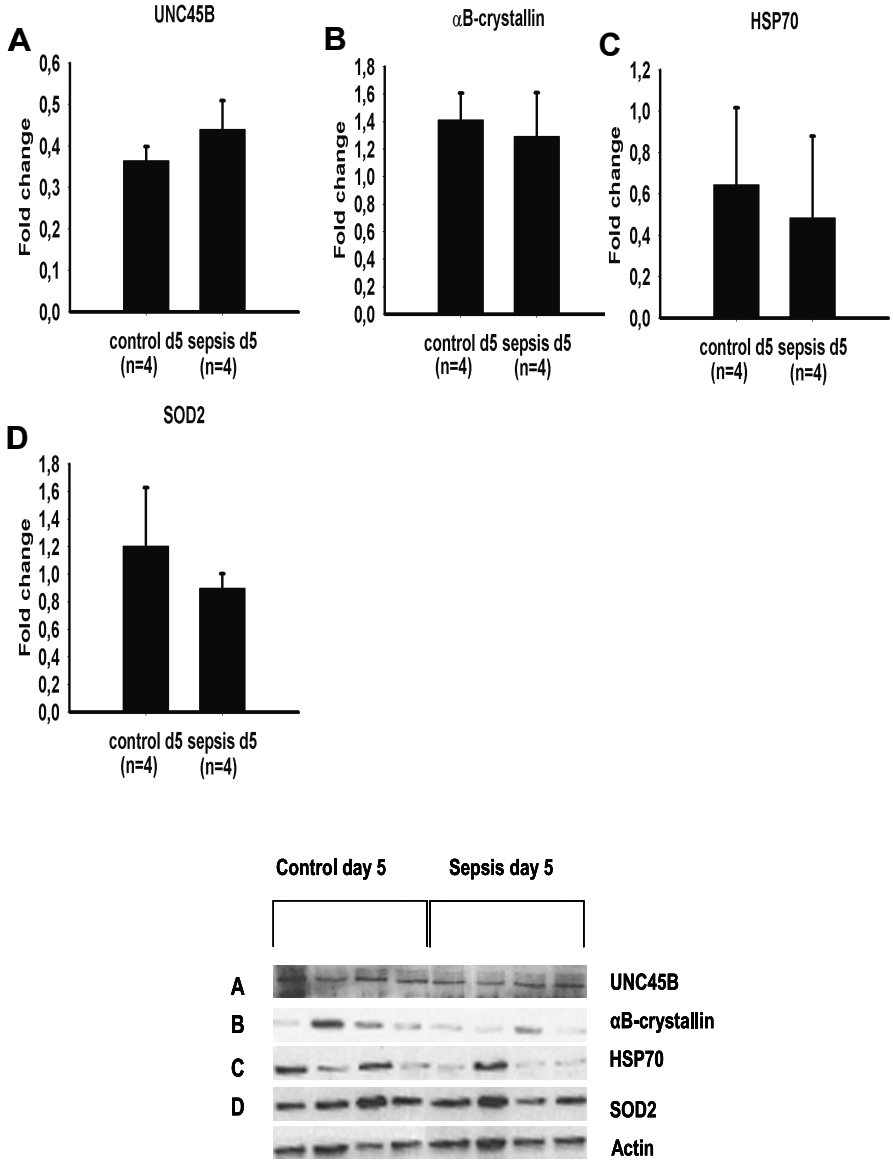

Figure 12. Western blot analyses in the biceps femoris muscle for the following proteins: UNC45B (A), αB-crystallin (B), HSP70 (C), and SOD2 (D), normalized to Actin contents. Values are means ± S.E.M.

Results suggest that elevation of chemokine genes, especially MCP-1 may induce the contractile properties in hind limb muscles (62). Due to the damage caused by the sepsis induction, different transcriptional regulation and kinase activity genes involved in the myogenic differentiation and muscle growth were up-regulated. The up-regulation of CEBPB is consistent with previous reports in inflammatory muscle wasting conditions (7). MAPK

signaling pathway has been reported to be activated in ICU patients with AQM (26).

The down-regulation of several heat shock protein genes in response to sepsis is suggested to be a key factor underlying the impaired force generating capacity. In our previous gene expression studies (1, 8), the force generating capacity of single muscle fibers were maintained and at the same time we also observed heat shock protein genes especially HSP70 and αB-crystallin to be up-regulated several folds. The down regulation of the molecular motor protein myosin (MYH7) and MyBP-C, the dominant thick filament proteins will have a major role for the decreased force generating capacity. Further, several oxidative stress responsive genes were down-regulated. This is consistent with the global down-regulation of oxidative stress responsive genes and impaired mitochondrial biogenesis in critically ill ICU patients with sepsis (37). In contrast, these oxidative stress responsive genes were up-regulated and muscle fiber size and specific force were maintained in limb muscles from pigs exposed to the ICU intervention per se without sepsis and in the masseter muscle in animals exposed to the ICU intervention, neuromuscular blockade, corticosteroids and sepsis. Thus, the reduced oxidative stress response may accordingly play an important role for the impaired muscle function in the septic pigs by enhancing posttranslational protein modifications and degradation (Paper II).

Do corticosteroids play an important role in the limb muscle? (Paper III)

Animals were mechanically ventilated with or without systemically induced corticosteroids and gene profiling revealed significant differences between the two experimental groups. The up-regulated gene clusters include kinase activity, zinc ion binding, cell cycle regulation, transcriptional regulation and channel regulation.

The down-regulated gene clusters include heat shock proteins, kinase activity, cytoskeletal & sarcomeric, oxidative stress responsive and RNA processing. In accordance with microarray data, real time RT-PCR results show up-regulation of the following genes: ACVR2B (A) and 4EBP1 (B). Down-regulation was confirmed in: MYH7 (C), MAP1A (D) and SOD2 (E) (figure 13).

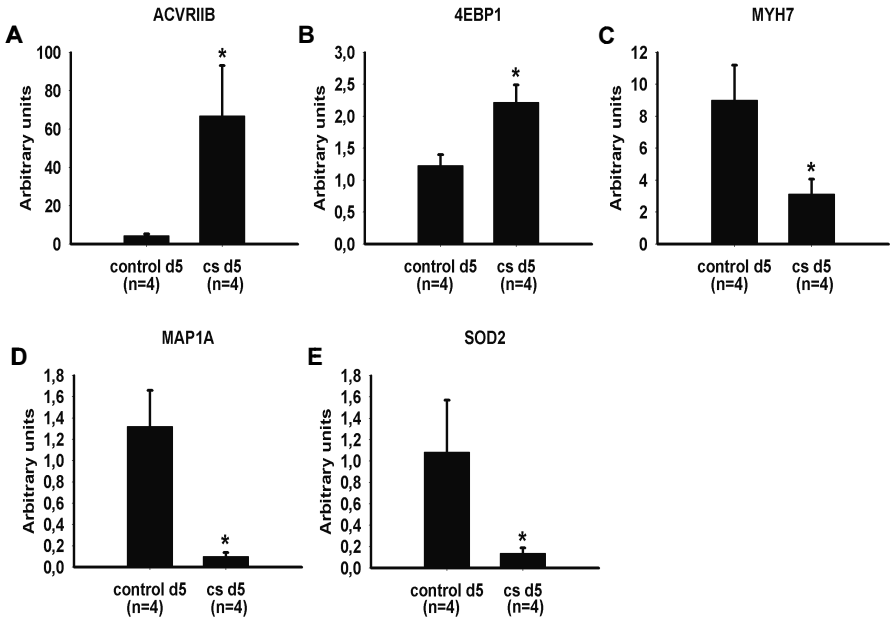

Figure 13. Microarray results were validated by real time RT-PCR in the biceps femoris muscle. ACVR2B (A) and 4EBP1 (B) were up-regulated, while MYH7 (C), MAP1A (D) and SOD2 (E) were down-regulated. Statistically significant differences versus the control group are denoted * ($p < 0.05$).

These results suggest an elevation of a number of kinase activity genes. MAPK signaling cascade along with TGF-β super family member ACVR2B up-regulation were observed. Similar observations like MAPK signaling and other members of the TGF-β receptor up-regulation have been reported in steroid induced patients (26). The cell cycle regulation genes GADD45 and P21 which act as downstream activators of MAPK signaling and involved in muscle fiber atrophy. Previously it has been shown that GADD45a induction can lead to skeletal muscle atrophy in fasting, immobilization and muscle denervation conditions (30). Furthermore, the increased myogenesis can be observed due to the up-regulation of cell cycle regulation genes including NR2F2, IL1RAP and BMP4. At the same time various transcriptional co-repressor genes like TLE1 and FHL3 were up-regulated, suggesting that these are involved in a negative muscle regulation. On the other hand, protein synthesis was also impaired in the corticosteroids group; this can be observed in the up-regulation of 4EBP1 gene and the down-regulation of EIF4E and eukaryotic translation initiation factor 3 subunit 3 (EIF3S3) genes. Previously it has been shown that glucocorticoids will attenuate the protein synthesis machinery by the up-regulation of 4EBP1, subsequently leading to decreased protein synthesis (130).

HSPs play an essential role during the stress recovery and at basal level these HSPs are acting as in-house chaperones. It is of specific interest to note that HSP70 down-regulation was observed in response to the ICU intervention together with corticosteroids compared with the ICU intervention alone. This result is consistent with our recent study, where HSP70 down-regulation was observed in response to the ICU intervention and sepsis compared with ICU intervention alone (2). Our previous gene array studies have indicated an up-regulation of HSP70 in the maintenance of muscle mass and function in the porcine ICU model (1, 8). HSP70 directly regulates skeletal muscle atrophy via FOXO signaling (127) and an inducible HSP70 over expression improves skeletal muscle structure and functional capacity (96).

The dominating thick filament protein, i.e., the molecular motor protein myosin (MYH7) has been reported to be down-regulated in response to the ICU intervention. However the further down-regulation of MYH7 when corticosteroids were added to the ICU intervention did not alter the myosin to actin ratio or fiber size, but was paralleled by a decline in specific force. In the rodent ICU model, longer exposure to immobilization, neuromuscular blockade, sedation and mechanical ventilation resulted in decreased actin and myosin mRNA expression, a preferential myosin loss, muscle fiber atrophy and decreased single fiber specific force, i.e., resembling the findings considered pathognomonic for the acquired myopathy observed in critically ill ICU patients (104). Different oxidative stress responsive genes like SOD2, and TXNRD1 were down-regulated. In our previous gene expression study these oxidative stress responsive genes were down-regulated in response to sepsis. On the other hand, the oxidative stress responsive genes were up-regulated in the masseter muscle of pigs; which were mechanically ventilated, sedated and treated with neuromuscular blockers, sepsis and corticosteroids for five days. However, muscle structure and function was maintained in the craniofacial muscle fibers in contrast to limb muscle fibers. Hence, the reduced oxidative stress may play an important role for the impaired muscle function in the corticosteroid treated pigs by enhancing post-translational protein modifications and degradation (Paper III).

Which factors trigger the diaphragm muscle dysfunction? (Paper IV)

In this study, pigs were exposed to different combinations of MV, endotoxin-induced sepsis, systemic administration of CS and NMBA for five days and compared with sham-operated control animals. Results indicated that there was no difference in fiber CSA, myosin heavy chain isoform proportion and contractile protein content of controls and animals treated for five days (figure 14B).

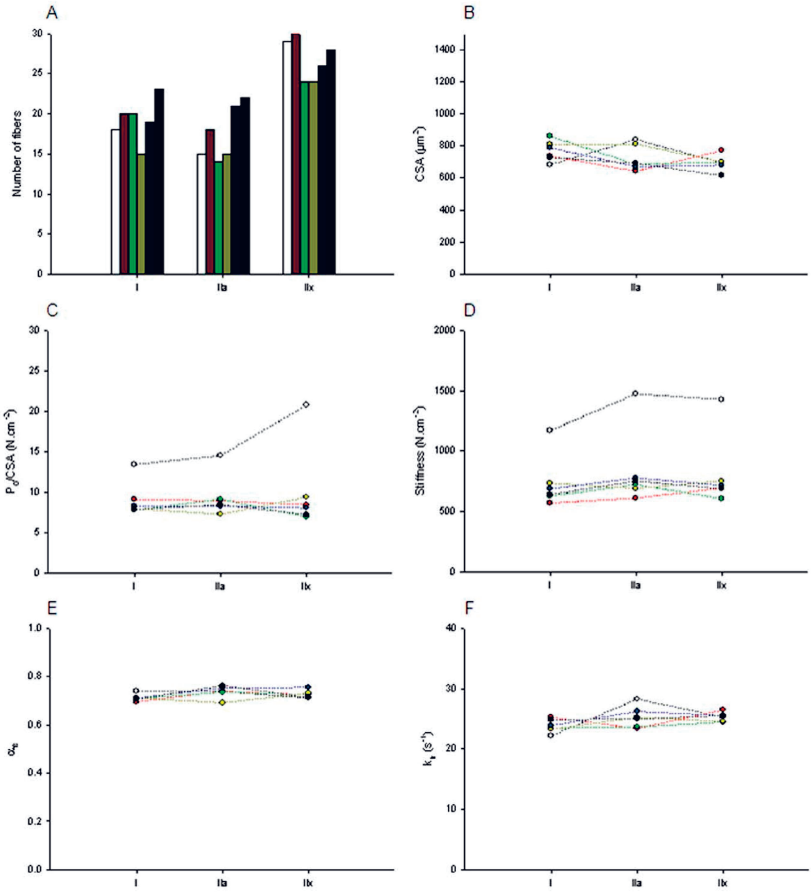

Figure 14. Fiber structure and function. A: Number of fibres tested. B: Cross-sectional area (CSA). C: Maximal force production normalized to CSA (P_0/CSA). D: Stiffness (E_0). E: Fraction of strongly attached cross-bridges (α_{fs}). F: Apparent rate constant of force redevelopment (k_{tr}). Values from CTL (white), MV (red bars), NMBA (green), CS (yellow), sepsis (blue) and ALL groups (black) appear. Data are presented as means.

However, a decrease in single fiber maximal force normalized to CSA (specific force) was observed in all experimental groups (figure 14C). The major loss in fiber stiffness (figure 14D) after five days of mechanical ventilation reveals a large decline in the number of myosin-actin interactions rather than a reduction in the force per cross-bridge interaction. The drop in the number of strongly attached cross-bridges is not related to dysfunction in the recruitment of myosin heads binding to actin (figure 14E) but to a decrease in functional myosin molecules. The sustained myosin and actin contents normalized to total protein content and total protein over cell volume reveals that the absolute content of contractile elements are not affected by the intervention.

The myosin and actin contents normalized to total protein content were preserved for all mechanically ventilated piglets (MV, sepsis, CS, NMBA and ALL groups) when compared with controls (figure 15B). In spite of large variability within each group, real time RT-PCR results indicate that type I MyHC isoform and actin mRNA levels were maintained. On the other hand, type IIx MyHC isoform mRNA expression was significantly decreased after five days for all mechanically ventilated groups (figure 15D).

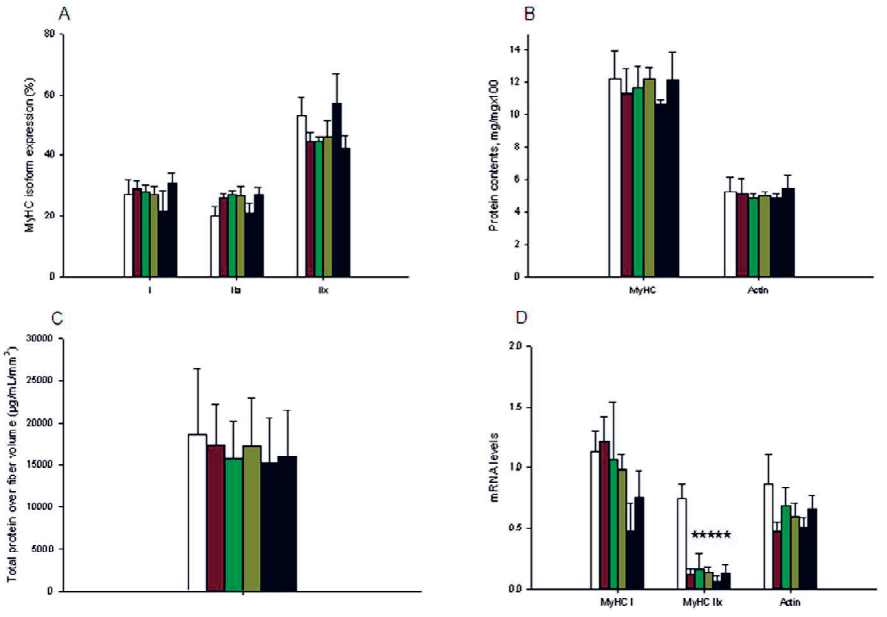

Figure 15. Protein and gene expressions. A: MyHC isoform composition. B: Contractile protein content. C: Total protein over fiber volume. D: mRNA levels of contractile proteins. Values from sham-operated control piglets (CTL group, white bars) and animals that were mechanically ventilated (MV group, red bars), mechanically ventilated with a neuromuscular blocking agent administration (NMBA group, green bars), mechanically ventilated with corticosteroid administration (CS group, yellow bars), mechanically ventilated with an injection of a endotoxin-induced sepsis (sepsis group, blue bars) and mechanically ventilated with a combination of endotoxin-induced sepsis, CS and NMBA (ALL group, black bars) for five days. Data are presented as means ± SEMs. Asterisk denotes a statistically significant difference compared with CTL ($p<0.05$).

There was no preferential loss of these contractile elements. To identify a potential general decline in the protein quantity per muscle fiber unit, the amount of total protein per fiber volume was estimated in a separate number of fibers. This amount was unchanged in all experimental piglets when compared with control animals. Oxidative modification of myosin and actin by

free radical species and other reactive species usually results in the formation of carbonyl groups into amino acid side chains by site-specific mechanism. These carbonyl groups or reactive carbonyl derivatives were identified for myosin and actin. Myosin oxidation was found unchanged whereas actin reactive carbonyl derivatives decreased after five days for all intervention groups (figure 16).

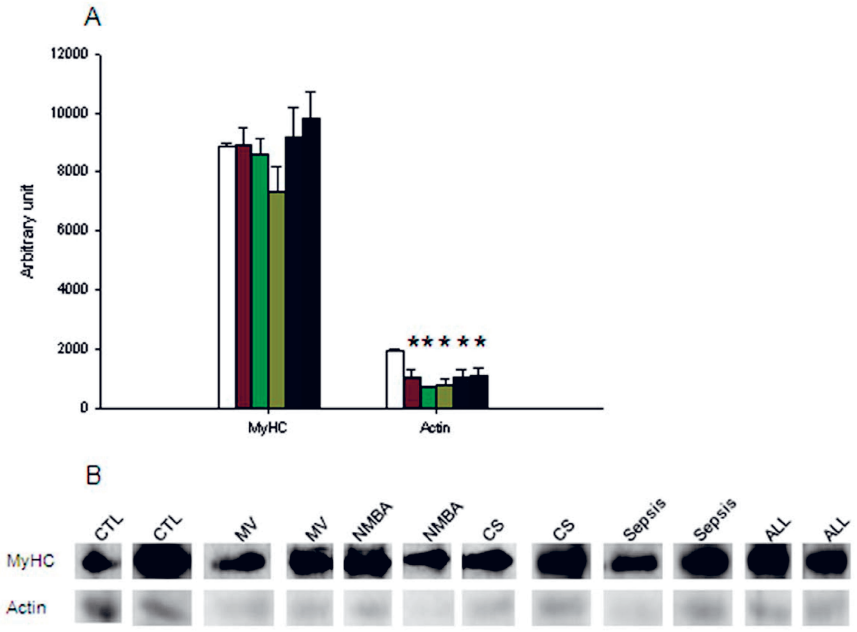

Figure 16. Contractile protein reactive carbonyl derivatives. A: CTL (white bars), MV (red bars), NMBA (green bars), CS (yellow bars), sepsis (blue bars) and ALL groups (black bars). B: Typical western blot showing reactive carbonyl derivates for various piglets. Data are presented as means ± SEMs. Asterisk denotes a statistically significant difference compared with CTL ($p<0.05$).

Even though a maintained diaphragm muscle fiber size after five days of mechanical ventilation and sedation, the maximum force decreased dramatically in membrane-permeabilized fibers expressing the type I, IIa and IIx MyHCs. The decreased specific force in response to five days of mechanical ventilation surely contributes to the impaired in vivo respiratory muscle function (110). Specific force is mainly determined by the number of strongly attached cross-bridges and the force produced by each cross-bridge.

Post-translational modifications of contractile proteins, resulting in an increased number of non-functional myosin or actin molecules, are forwarded as a probable mechanism underlying the decreased specific force in response

to MV and sedation. This is in agreement with previous studies showing a significant increase in myosin and actin carbonylation in response to one to two days of mechanical ventilation (149). However, five days of mechanical ventilation and sedation did not show increased amount of carbonyl derivatives, instead a decreased amount of C = O in actin molecules was observed for pigs exposed to mechanical ventilation for five days with or without CS, NMBA and sepsis.

Severe muscle wasting and impaired diaphragm muscle function is observed in critically ill ICU patients, delaying weaning from the respirator. The present results reveal that five days of mechanical ventilation cause a severe diaphragm muscle fiber dysfunction without any major structural remodeling at the cell and protein levels. Surprisingly, sepsis, CS and NMBA, examined separately or in combination, do not add significant negative effects to the ventilator-induced diaphragm changes. (Paper IV).

Conclusions

Acute quadriplegic myopathy (AQM) is a common neuromuscular disorder in critically ill intensive care unit (ICU) patients. AQM patients have persistent, moderate or severe, flaccid generalized weakness and muscle becomes atrophic. Distal and proximal muscles may be affected equally, but distal weakness occasionally predominates. Craniofacial (masseter) muscles are, on the other hand, less or not affected, while respiratory function is typically severely impaired. Mechanical ventilation (MV), immobilization, neuromuscular blocking agents (NMBA), corticosteroids (CS) and sepsis have been forwarded as the main factors triggering AQM. A unique porcine model was used to study the impact of these triggering factors on skeletal muscle and more specifically on difference between muscle types i.e., between limb, respiratory and craniofacial muscles.

Masseter and biceps femoris muscle gene expression profiling experiments were conducted to unravel the molecular mechanisms underlying the sparing of the craniofacial versus limb muscles. Microarray data revealed 825 genes in masseter and 1240 genes in the biceps femoris muscle that were deregulated, furthermore in accordance with results from limb muscles, the proteolytic pathway genes (UPS and ALP) were seen to be up-regulated. However, in contrast to limb muscles, the protein protective mechanisms genes (HSPs and TIMP 2) were up-regulated and the negative regulator of the muscle growth, the myostatin gene, was down-regulated in the masticatory muscle. This resulted in maintained single masseter muscle fiber CSA and the force generation capacity (specific force) in single muscle fibers, in contrast to the dramatic decline observed in limb single muscle fiber specific force.

Biceps femoris muscle gene expression profiling experiments were also conducted to unravel the role of sepsis in the development of limb muscle weakness in a porcine ICU model. Results highlighted that on day five, muscle fiber size did not differ between the sepsis and MV groups. However, a significant decrease in the single fiber maximal force normalized to cross-sectional area (specific force) was observed in the sepsis group when compared with the MV group. In addition, microarray data showed a deregulation of more than 500 genes, such as an increased expression of genes involved in chemokine activity, kinase activity and transcriptional regulation. Furthermore an observed decreased expression in heat shock, oxidative stress response, cytoskeletal and sarcomeric genes was also apparent. Sepsis-

induced changes in the gene expression of chemokine activity and heat shock proteins are forwarded as critical factors underlying the decreased force generating capacity at the single fiber level. By targeting these genes, future experiments can give an insight into the development of innovative treatments expected at protecting muscle mass and function in critically ill ICU patients.

Gene expression profiling experiments were conducted in the biceps femoris muscle to unravel the effects of corticosteroids in the development of limb muscle weakness in a porcine ICU model. Results highlighted that on day five, muscle fiber size did not differ between corticosteroids and MV groups. However, a significant decrease in the single fiber maximal force normalized to cross-sectional area (specific force) was observed in the corticosteroids group when compared to the MV group. In addition, microarray data showed a deregulation of 186 genes, such as an increased expression of genes involved in kinase activity and transcriptional regulation. Furthermore a decreased expression in heat shock, oxidative stress response, cytoskeletal and sarcomeric genes was also apparent. Systemic corticosteroid-induced changes in the gene expression of kinase activity and heat shock proteins are forwarded as critical factors underlying the decreased force generating capacity at the single fiber level. By targeting these genes future experiments can provide an important clinical avenue aiming at protecting muscle mass and function in critically ill ICU patients.

In the diaphragm, morphological and biochemical analyses demonstrate and intact muscle fiber structure (myosin heavy chain isoform proportion, cross-sectional area (CSA) and contractile protein content) after five days exposure to MV and sedation alone or in combination with NMBA, CS and sepsis. However, a decrease in single fiber maximal force normalized to CSA (specific force) was observed in all piglets. Unexpectedly, sepsis, CS or NMBA did not have any significant additive effects, suggesting that MV is the main factor triggering diaphragm weakness.

Acknowledgments

This work was carried out at the Clinical Neurophysiology, Department of Neuroscience, Uppsala University, Uppsala, Sweden in collaboration with research groups at the Department of Medical sciences, Uppsala University, Uppsala, Sweden; Department of Anesthesiology, Karolinska Institute, Stockholm, Sweden; Research Center for Genetic Medicine, Children National Medical Center Washington, District of Columbia; Department of Pediatrics, The George Washington University Medical Center, Washington, District of Columbia; Department of Biobehavioral Health, The Pennsylvania State University, University Park, PA, USA.

I would like to thank many people who directly or indirectly contributed to the completion of this thesis.

I would like to thank my supervisor, Professor Lars Larsson, who has introduced me to the exciting field of skeletal muscle research. I am very grateful for all the guidance and support that he has given me over all these years. He is a real role model for a hardworking scientist. In ancient Indian tradition we have special respect to Guru (teacher), which is beautifully quoted in Sanskrit hymn “acharya devo bhava". This is the belief I believed and experienced throughout my life.

I would like to thank my co-supervisor, Dr. Julien Ochala, you are simply amazing and for all the help you extended to me whenever I needed it.

I would specially like to acknowledge my collaborators from the Karolinska Institute Professor Peter Radell and Lars I Eriksson; and from the Department of Medical sciences Dr. Hanna Göransson; and from the Research Center for Genetic Medicine, Children National Medical Center Washington, District of Columbia, US, Professor Eric Hoffman and Dr. Yi-Wen Chen.
This work would not have been possible without your support.

My group members have always been like one big family for me, always there to help whenever I needed. I thank all the present members Ann-Marie Gustafson, Yvette Hedström, Meishan Li, Rebeca Corpeño, Guillaume Renaud, Johan Lindqvist, Nicola Cacciani, Hannah Ogilvie, Maria Wilen, Hazem Aqqad and former members Rizwan Qaisar, Monica Llano-Diez, Varu-

na Banduseela, Andreas Ruden, Marit De Haan (for nice cakes) and Ayse Malci. Special thanks to Hannah Ogilvie for helping me with English editing. I would like to thank Inger Hedlund & Gun Schönnings for administrative help, David and Peo for helping with computer and printer problems.

My special thanks to Dr. Karin & Professor Orvar for your help and friendship all these years.

I would like to thank all staff at Clinical Neurophysiology. I am grateful to each one of you for your warm welcome, hospitality and help.

Special thanks to Madhu Bysani for introducing me to this department. I also thank all my friends in Sweden: Saveer, Vijay, Srisailam, Srivatsa, Prasad, Mukunda, Kiran K, Chandu, Ramesh, Ravi, Kiran J, Arjun, Rambabu, Raghuveer, Rajesh, Srikanth, Satyam, Mayank, Vamshi, Vivek, Shamraj, Gayathri, Geetha, Madhuri, Laura, Vijaya, Swathi, Sushma, Bhavya, Laxmi, and Divya for their friendship.

I would like to thank one special person Sir B V Rao garu, for his extended support whenever I needed it and also thanks to all my teachers. I want to thank all my friends and well wishers in India especially Mathiyarasu, Rajender, Venkatesh, Jagadish, Chandra Kiran, Balaram, Srinu, and Jayadev.

I can never forget all the love, affection and support that I got over the years from my parents, brother, sister, family and my wife's family.

One of the most important people in my life is my wife Saritha, for trying to understand me and helping me in every possible way, I will always love you.

Finally, to my little angel Sanvika for bringing joy into our families lives.

References

1. **Aare S, Ochala J, Norman HS, Radell P, Eriksson LI, Goransson H, Chen YW, Hoffman EP, and Larsson L**. Mechanisms underlying the sparing of masticatory versus limb muscle function in an experimental critical illness model. *Physiol Genomics* 43: 1334-1350, 2011.
2. **Aare S, Radell P, Eriksson LI, Chen YW, Hoffman EP, and Larsson L**. The role of sepsis in the development of limb muscle weakness in a porcine intensive care unit model. *Physiol Genomics* 2012 44: 865-877.
3. **Alamdari N, Aversa Z, Castillero E, Gurav A, Petkova V, Tizio S, and Hasselgren PO**. Resveratrol prevents dexamethasone-induced expression of the muscle atrophy-related ubiquitin ligases atrogin-1 and MuRF1 in cultured myotubes through a SIRT1-dependent mechanism. *Biochem Biophys Res Commun* 417: 528-533, 2012.
4. **Ali MA, Cho WJ, Hudson B, Kassiri Z, Granzier H, and Schulz R**. Titin is a target of matrix metalloproteinase-2: implications in myocardial ischemia/reperfusion injury. *Circulation* 122: 2039-2047, 2010.
5. **Arany Z, Lebrasseur N, Morris C, Smith E, Yang W, Ma Y, Chin S, and Spiegelman BM**. The transcriptional coactivator PGC-1beta drives the formation of oxidative type IIX fibers in skeletal muscle. *Cell Metab* 5: 35-46, 2007.
6. **Arner ES, and Holmgren A**. Physiological functions of thioredoxin and thioredoxin reductase. *Eur J Biochem* 267: 6102-6109, 2000.
7. **Aversa Z, Alamdari N, and Hasselgren PO**. Molecules modulating gene transcription during muscle wasting in cancer, sepsis, and other critical illness. *Crit Rev Clin Lab Sci* 48: 71-86, 2011.
8. **Banduseela VC, Ochala J, Chen YW, Goransson H, Norman H, Radell P, Eriksson LI, Hoffman EP, and Larsson L**. Gene expression and muscle fiber function in a porcine ICU model. *Physiol Genomics* 39: 141-159, 2009.
9. **Bartoli M, and Richard I**. Calpains in muscle wasting. *Int J Biochem Cell Biol* 37: 2115-2133, 2005.
10. **Bechet D, Tassa A, Taillandier D, Combaret L, and Attaix D**. Lysosomal proteolysis in skeletal muscle. *Int J Biochem Cell Biol* 37: 2098-2114, 2005.
11. **Bodine SC, Latres E, Baumhueter S, Lai VK, Nunez L, Clarke BA, Poueymirou WT, Panaro FJ, Na E, Dharmarajan K, Pan ZQ, Valenzuela DM, DeChiara TM, Stitt TN, Yancopoulos GD, and Glass DJ**. Identification of ubiquitin ligases required for skeletal muscle atrophy. *Science* 294: 1704-1708, 2001.
12. **Bodine SC, Stitt TN, Gonzalez M, Kline WO, Stover GL, Bauerlein R, Zlotchenko E, Scrimgeour A, Lawrence JC, Glass DJ, and Yancopoulos GD**. Akt/mTOR pathway is a crucial regulator of skeletal muscle hypertrophy and can prevent muscle atrophy in vivo. *Nat Cell Biol* 3: 1014-1019, 2001.

13. **Bolton CF**. Neuromuscular manifestations of critical illness. *Muscle Nerve* 32: 140-163, 2005.
14. **Brealey D, Brand M, Hargreaves I, Heales S, Land J, Smolenski R, Davies NA, Cooper CE, and Singer M**. Association between mitochondrial dysfunction and severity and outcome of septic shock. *Lancet* 360: 219-223, 2002.
15. **Buckingham M, and Relaix F**. The role of Pax genes in the development of tissues and organs: Pax3 and Pax7 regulate muscle progenitor cell functions. *Annu Rev Cell Dev Biol* 23: 645-673, 2007.
16. **Cai D, Frantz JD, Tawa NE, Jr., Melendez PA, Oh BC, Lidov HG, Hasselgren PO, Frontera WR, Lee J, Glass DJ, and Shoelson SE**. IKKbeta/NF-kappaB activation causes severe muscle wasting in mice. *Cell* 119: 285-298, 2004.
17. **Caiozzo VJ**. Plasticity of skeletal muscle phenotype: mechanical consequences. *Muscle Nerve* 26: 740-768, 2002.
18. **Canicio J, Ruiz-Lozano P, Carrasco M, Palacin M, Chien K, Zorzano A, and Kaliman P**. Nuclear factor kappa B-inducing kinase and Ikappa B kinase-alpha signal skeletal muscle cell differentiation. *J Biol Chem* 276: 20228-20233, 2001.
19. **Carmeli E, Moas M, Reznick AZ, and Coleman R**. Matrix metalloproteinases and skeletal muscle: a brief review. *Muscle Nerve* 29: 191-197, 2004.
20. **Chen YW, Zhao P, Borup R, and Hoffman EP**. Expression profiling in the muscular dystrophies: identification of novel aspects of molecular pathophysiology. *J Cell Biol* 151: 1321-1336, 2000.
21. **Cohen S, Brault JJ, Gygi SP, Glass DJ, Valenzuela DM, Gartner C, Latres E, and Goldberg AL**. During muscle atrophy, thick, but not thin, filament components are degraded by MuRF1-dependent ubiquitylation. *J Cell Biol* 185: 1083-1095, 2009.
22. **Davidson TA, Caldwell ES, Curtis JR, Hudson LD, and Steinberg KP**. Reduced quality of life in survivors of acute respiratory distress syndrome compared with critically ill control patients. *JAMA* 281: 354-360, 1999.
23. **De Jonghe B, Bastuji-Garin S, Sharshar T, Outin H, and Brochard L**. Does ICU-acquired paresis lengthen weaning from mechanical ventilation? *Intensive Care Med* 30: 1117-1121, 2004.
24. **De Jonghe B, Sharshar T, Lefaucheur JP, Authier FJ, Durand-Zaleski I, Boussarsar M, Cerf C, Renaud E, Mesrati F, Carlet J, Raphael JC, Outin H, and Bastuji-Garin S**. Paresis acquired in the intensive care unit: a prospective multicenter study. *JAMA* 288: 2859-2867, 2002.
25. **De Paepe B, Creus KK, Martin JJ, Weis J, and De Bleecker JL**. A dual role for HSP90 and HSP70 in the inflammatory myopathies: from muscle fiber protection to active invasion by macrophages. *Ann N Y Acad Sci* 1173: 463-469, 2009.
26. **Di Giovanni S, Molon A, Broccolini A, Melcon G, Mirabella M, Hoffman EP, and Servidei S**. Constitutive activation of MAPK cascade in acute quadriplegic myopathy. *Ann Neurol* 55: 195-206, 2004.
27. **Djabali K, de Nechaud B, Landon F, and Portier MM**. AlphaB-crystallin interacts with intermediate filaments in response to stress. *J Cell Sci* 110 (Pt 21): 2759-2769, 1997.
28. **Dodd SL, Hain B, Senf SM, and Judge AR**. Hsp27 inhibits IKKbeta-induced NF-kappaB activity and skeletal muscle atrophy. *FASEB J* 23: 3415-3423, 2009.

29. **Douglass JA, Tuxen DV, Horne M, Scheinkestel CD, Weinmann M, Czarny D, and Bowes G**. Myopathy in severe asthma. *Am Rev Respir Dis* 146: 517-519, 1992.
30. **Ebert SM, Dyle MC, Kunkel SD, Bullard SA, Bongers KS, Fox DK, Dierdorff JM, Foster ED, and Adams CM**. Stress-induced skeletal muscle Gadd45a expression reprograms myonuclei and causes muscle atrophy. *J Biol Chem* 2012.
31. **Edman KA**. The velocity of unloaded shortening and its relation to sarcomere length and isometric force in vertebrate muscle fibres. *J Physiol* 291: 143-159, 1979.
32. **Eriksson PO, and Thornell LE**. Histochemical and morphological muscle-fibre characteristics of the human masseter, the medial pterygoid and the temporal muscles. *Arch Oral Biol* 28: 781-795, 1983.
33. **Fabiato A**. Computer programs for calculating total from specified free or free from specified total ionic concentrations in aqueous solutions containing multiple metals and ligands. *Methods Enzymol* 157: 378-417, 1988.
34. **Fan E, Zanni JM, Dennison CR, Lepre SJ, and Needham DM**. Critical illness neuromyopathy and muscle weakness in patients in the intensive care unit. *AACN Adv Crit Care* 20: 243-253, 2009.
35. **Fernandez AM, Dupont J, Farrar RP, Lee S, Stannard B, and Le Roith D**. Muscle-specific inactivation of the IGF-I receptor induces compensatory hyperplasia in skeletal muscle. *J Clin Invest* 109: 347-355, 2002.
36. **Figliola R, Busanello A, Vaccarello G, and Maione R**. Regulation of p57(KIP2) during muscle differentiation: role of Egr1, Sp1 and DNA hypomethylation. *J Mol Biol* 380: 265-277, 2008.
37. **Fredriksson K, Tjader I, Keller P, Petrovic N, Ahlman B, Scheele C, Wernerman J, Timmons JA, and Rooyackers O**. Dysregulation of mitochondrial dynamics and the muscle transcriptome in ICU patients suffering from sepsis induced multiple organ failure. *PLoS One* 3: e3686, 2008.
38. **Frontera WR, and Larsson L**. Contractile studies of single human skeletal muscle fibers: a comparison of different muscles, permeabilization procedures, and storage techniques. *Muscle Nerve* 20: 948-952, 1997.
39. **Glass DJ**. Skeletal muscle hypertrophy and atrophy signaling pathways. *Int J Biochem Cell Biol* 37: 1974-1984, 2005.
40. **Goldfarb LG, and Dalakas MC**. Tragedy in a heartbeat: malfunctioning desmin causes skeletal and cardiac muscle disease. *J Clin Invest* 119: 1806-1813, 2009.
41. **Goll DE, Thompson VF, Li H, Wei W, and Cong J**. The calpain system. *Physiol Rev* 83: 731-801, 2003.
42. **Gomes MD, Lecker SH, Jagoe RT, Navon A, and Goldberg AL**. Atrogin-1, a muscle-specific F-box protein highly expressed during muscle atrophy. *Proc Natl Acad Sci U S A* 98: 14440-14445, 2001.
43. **Gonnella P, Alamdari N, Tizio S, Aversa Z, Petkova V, and Hasselgren PO**. C/EBPbeta regulates dexamethasone-induced muscle cell atrophy and expression of atrogin-1 and MuRF1. *J Cell Biochem* 112: 1737-1748, 2011.
44. **Granlund A, Jensen-Waern M, and Essen-Gustavsson B**. The influence of the PRKAG3 mutation on glycogen, enzyme activities and fibre types in different skeletal muscles of exercise trained pigs. *Acta Vet Scand* 53: 20, 2011.
45. **Griffiths RD, and Hall JB**. Intensive care unit-acquired weakness. *Crit Care Med* 38: 779-787.

46. **Grifone R, and Kelly RG**. Heartening news for head muscle development. *Trends Genet* 23: 365-369, 2007.
47. **Grumati P, Coletto L, Sabatelli P, Cescon M, Angelin A, Bertaggia E, Blaauw B, Urciuolo A, Tiepolo T, Merlini L, Maraldi NM, Bernardi P, Sandri M, and Bonaldo P**. Autophagy is defective in collagen VI muscular dystrophies, and its reactivation rescues myofiber degeneration. *Nat Med* 16: 1313-1320.
48. **Haddad F, Roy RR, Zhong H, Edgerton VR, and Baldwin KM**. Atrophy responses to muscle inactivity. II. Molecular markers of protein deficits. *J Appl Physiol* 95: 791-802, 2003.
49. **Hawke TJ, Meeson AP, Jiang N, Graham S, Hutcheson K, DiMaio JM, and Garry DJ**. p21 is essential for normal myogenic progenitor cell function in regenerating skeletal muscle. *Am J Physiol Cell Physiol* 285: C1019-1027, 2003.
50. **Hentschke M, and Borgmeyer U**. Identification of PNRC2 and TLE1 as activation function-1 cofactors of the orphan nuclear receptor ERRgamma. *Biochem Biophys Res Commun* 312: 975-982, 2003.
51. **Hirota K, Murata M, Sachi Y, Nakamura H, Takeuchi J, Mori K, and Yodoi J**. Distinct roles of thioredoxin in the cytoplasm and in the nucleus. A two-step mechanism of redox regulation of transcription factor NF-kappaB. *J Biol Chem* 274: 27891-27897, 1999.
52. **Holmes BF, Sparling DP, Olson AL, Winder WW, and Dohm GL**. Regulation of muscle GLUT4 enhancer factor and myocyte enhancer factor 2 by AMP-activated protein kinase. *Am J Physiol Endocrinol Metab* 289: E1071-1076, 2005.
53. **Hsieh CM, Fukumoto S, Layne MD, Maemura K, Charles H, Patel A, Perrella MA, and Lee ME**. Striated muscle preferentially expressed genes alpha and beta are two serine/threonine protein kinases derived from the same gene as the aortic preferentially expressed gene-1. *J Biol Chem* 275: 36966-36973, 2000.
54. **Huang da W, Sherman BT, Tan Q, Collins JR, Alvord WG, Roayaei J, Stephens R, Baseler MW, Lane HC, and Lempicki RA**. The DAVID Gene Functional Classification Tool: a novel biological module-centric algorithm to functionally analyze large gene lists. *Genome Biol* 8: R183, 2007.
55. **Huxley HE**. The mechanism of muscular contraction. *Science* 164: 1356-1365, 1969.
56. **Irizarry RA, Hobbs B, Collin F, Beazer-Barclay YD, Antonellis KJ, Scherf U, and Speed TP**. Exploration, normalization, and summaries of high density oligonucleotide array probe level data. *Biostatistics* 4: 249-264, 2003.
57. **Janssen E, de Groof A, Wijers M, Fransen J, Dzeja PP, Terzic A, and Wieringa B**. Adenylate kinase 1 deficiency induces molecular and structural adaptations to support muscle energy metabolism. *J Biol Chem* 278: 12937-12945, 2003.
58. **Jiang L, Chen Y, Chan CY, Lu G, Wang H, Li JC, and Kung HF**. Dynamic transcriptional changes of TIEG1 and TIEG2 during mouse tissue development. *Anat Rec (Hoboken)* 293: 858-864, 2010.
59. **Kelly RG, Jerome-Majewska LA, and Papaioannou VE**. The del22q11.2 candidate gene Tbx1 regulates branchiomeric myogenesis. *Hum Mol Genet* 13: 2829-2840, 2004.
60. **Klionsky DJ**. The molecular machinery of autophagy: unanswered questions. *J Cell Sci* 118: 7-18, 2005.

61. **Kurabe N, Mori M, Kurokawa J, Taniguchi K, Aoyama H, Atsuda K, Nishijima A, Odawara N, Harada S, Nakashima K, Arai S, and Miyazaki T**. The death effector domain-containing DEDD forms a complex with Akt and Hsp90, and supports their stability. *Biochem Biophys Res Commun* 391: 1708-1713, 2010.
62. **Labbe K, Danialou G, Gvozdic D, Demoule A, Divangahi M, Boyd JH, and Petrof BJ**. Inhibition of monocyte chemoattractant protein-1 prevents diaphragmatic inflammation and maintains contractile function during endotoxemia. *Crit Care* 14: R187, 2010.
63. **Lacomis D, Petrella JT, and Giuliani MJ**. Causes of neuromuscular weakness in the intensive care unit: a study of ninety-two patients. *Muscle Nerve* 21: 610-617, 1998.
64. **Lacomis D, Zochodne DW, and Bird SJ**. Critical illness myopathy. *Muscle Nerve* 23: 1785-1788, 2000.
65. **Langlands K, Yin X, Anand G, and Prochownik EV**. Differential interactions of Id proteins with basic-helix-loop-helix transcription factors. *J Biol Chem* 272: 19785-19793, 1997.
66. **Larsson L**. Experimental animal models of muscle wasting in intensive care unit patients. *Crit Care Med* 35: S484-487, 2007.
67. **Larsson L, Ansved T, Edstrom L, Gorza L, and Schiaffino S**. Effects of age on physiological, immunohistochemical and biochemical properties of fast-twitch single motor units in the rat. *J Physiol* 443: 257-275, 1991.
68. **Larsson L, Biral D, Campione M, and Schiaffino S**. An age-related type IIB to IIX myosin heavy chain switching in rat skeletal muscle. *Acta Physiol Scand* 147: 227-234, 1993.
69. **Larsson L, Li X, Edstrom L, Eriksson LI, Zackrisson H, Argentini C, and Schiaffino S**. Acute quadriplegia and loss of muscle myosin in patients treated with nondepolarizing neuromuscular blocking agents and corticosteroids: mechanisms at the cellular and molecular levels. *Crit Care Med* 28: 34-45, 2000.
70. **Larsson L, and Moss RL**. Maximum velocity of shortening in relation to myosin isoform composition in single fibres from human skeletal muscles. *J Physiol* 472: 595-614, 1993.
71. **Larsson L, and Roland A**. [Drug induced tetraparesis and loss of myosin. Mild types are probably overlooked]. *Lakartidningen* 93: 2249-2254, 1996.
72. **Larsson L, Yu F, Hook P, Ramamurthy B, Marx JO, and Pircher P**. Effects of aging on regulation of muscle contraction at the motor unit, muscle cell, and molecular levels. *Int J Sport Nutr Exerc Metab* 11 Suppl: S28-43, 2001.
73. **Latronico N, and Bolton CF**. Critical illness polyneuropathy and myopathy: a major cause of muscle weakness and paralysis. *Lancet Neurol* 10: 931-941, 2011.
74. **Lecker SH, Jagoe RT, Gilbert A, Gomes M, Baracos V, Bailey J, Price SR, Mitch WE, and Goldberg AL**. Multiple types of skeletal muscle atrophy involve a common program of changes in gene expression. *FASEB J* 18: 39-51, 2004.
75. **Lecomte V, Meugnier E, Euthine V, Durand C, Freyssenet D, Nemoz G, Rome S, Vidal H, and Lefai E**. A new role for sterol regulatory element binding protein 1 transcription factors in the regulation of muscle mass and muscle cell differentiation. *Mol Cell Biol* 30: 1182-1198, 2010.

76. **Leijten FS, Harinck-de Weerd JE, Poortvliet DC, and de Weerd AW**. The role of polyneuropathy in motor convalescence after prolonged mechanical ventilation. *JAMA* 274: 1221-1225, 1995.
77. **Lepper C, Conway SJ, and Fan CM**. Adult satellite cells and embryonic muscle progenitors have distinct genetic requirements. *Nature* 460: 627-631, 2009.
78. **Lescroart F, Kelly RG, Le Garrec JF, Nicolas JF, Meilhac SM, and Buckingham M**. Clonal analysis reveals common lineage relationships between head muscles and second heart field derivatives in the mouse embryo. *Development* 137: 3269-3279.
79. **Levine B, and Kroemer G**. Autophagy in the pathogenesis of disease. *Cell* 132: 27-42, 2008.
80. **Levine S, Nguyen T, Taylor N, Friscia ME, Budak MT, Rothenberg P, Zhu J, Sachdeva R, Sonnad S, Kaiser LR, Rubinstein NA, Powers SK, and Shrager JB**. Rapid disuse atrophy of diaphragm fibers in mechanically ventilated humans. *N Engl J Med* 358: 1327-1335, 2008.
81. **Li C, and Wong WH**. Model-based analysis of oligonucleotide arrays: expression index computation and outlier detection. *Proc Natl Acad Sci U S A* 98: 31-36, 2001.
82. **Li YP, Chen Y, John J, Moylan J, Jin B, Mann DL, and Reid MB**. TNF-alpha acts via p38 MAPK to stimulate expression of the ubiquitin ligase atrogin1/MAFbx in skeletal muscle. *FASEB J* 19: 362-370, 2005.
83. **Lindstrom M, Pedrosa-Domellof F, and Thornell LE**. Satellite cell heterogeneity with respect to expression of MyoD, myogenin, Dlk1 and c-Met in human skeletal muscle: application to a cohort of power lifters and sedentary men. *Histochem Cell Biol* 134: 371-385, 2010.
84. **MacFarlane IA, and Rosenthal FD**. Severe myopathy after status asthmaticus. *Lancet* 2: 615, 1977.
85. **Martin AF**. Turnover of cardiac troponin subunits. Kinetic evidence for a precursor pool of troponin-I. *J Biol Chem* 256: 964-968, 1981.
86. **Martyn DA, Smith L, Kreutziger KL, Xu S, Yu LC, and Regnier M**. The effects of force inhibition by sodium vanadate on cross-bridge binding, force redevelopment, and Ca2+ activation in cardiac muscle. *Biophys J* 92: 4379-4390, 2007.
87. **Masiero E, Agatea L, Mammucari C, Blaauw B, Loro E, Komatsu M, Metzger D, Reggiani C, Schiaffino S, and Sandri M**. Autophagy is required to maintain muscle mass. *Cell Metab* 10: 507-515, 2009.
88. **Massa R, Carpenter S, Holland P, and Karpati G**. Loss and renewal of thick myofilaments in glucocorticoid-treated rat soleus after denervation and reinnervation. *Muscle Nerve* 15: 1290-1298, 1992.
89. **Matsumoto N, Nakamura T, Yasui Y, and Torii J**. Analysis of muscle proteins in acute quadriplegic myopathy. *Muscle Nerve* 23: 1270-1276, 2000.
90. **McArdle A, Broome CS, Kayani AC, Tully MD, Close GL, Vasilaki A, and Jackson MJ**. HSF expression in skeletal muscle during myogenesis: implications for failed regeneration in old mice. *Exp Gerontol* 41: 497-500, 2006.
91. **McCroskery S, Thomas M, Maxwell L, Sharma M, and Kambadur R**. Myostatin negatively regulates satellite cell activation and self-renewal. *J Cell Biol* 162: 1135-1147, 2003.
92. **McDonald KS, and Fitts RH**. Effect of hindlimb unloading on rat soleus fiber force, stiffness, and calcium sensitivity. *J Appl Physiol* 79: 1796-1802, 1995.

93. **McNicol FJ, Hoyland JA, Cooper RG, and Carlson GL**. Skeletal muscle contractile properties and proinflammatory cytokine gene expression in human endotoxaemia. *Br J Surg* 97: 434-442, 2010.
94. **McPherron AC, Lawler AM, and Lee SJ**. Regulation of skeletal muscle mass in mice by a new TGF-beta superfamily member. *Nature* 387: 83-90, 1997.
95. **Melchionna R, Di Carlo A, De Mori R, Cappuzzello C, Barberi L, Musaro A, Cencioni C, Fujii N, Tamamura H, Crescenzi M, Capogrossi MC, Napolitano M, and Germani A**. Induction of myogenic differentiation by SDF-1 via CXCR4 and CXCR7 receptors. *Muscle Nerve* 41: 828-835, 2010.
96. **Miyabara EH, Nascimento TL, Rodrigues DC, Moriscot AS, Davila WF, AitMou Y, deTombe PP, and Mestril R**. Overexpression of inducible 70-kDa heat shock protein in mouse improves structural and functional recovery of skeletal muscles from atrophy. *Pflugers Arch* 463: 733-741, 2012.
97. **Mizushima N, Levine B, Cuervo AM, and Klionsky DJ**. Autophagy fights disease through cellular self-digestion. *Nature* 451: 1069-1075, 2008.
98. **Monemi M, Kadi F, Liu JX, Thornell LE, and Eriksson PO**. Adverse changes in fibre type and myosin heavy chain compositions of human jaw muscle vs. limb muscle during ageing. *Acta Physiol Scand* 167: 339-345, 1999.
99. **Moss RL**. Sarcomere length-tension relations of frog skinned muscle fibres during calcium activation at short lengths. *J Physiol* 292: 177-192, 1979.
100. **Ni Z, and Storey KB**. Heme oxygenase expression and Nrf2 signaling during hibernation in ground squirrels. *Can J Physiol Pharmacol* 88: 379-387, 2010.
101. **Noden DM, and Francis-West P**. The differentiation and morphogenesis of craniofacial muscles. *Dev Dyn* 235: 1194-1218, 2006.
102. **Norman H, Kandala K, Kolluri R, Zackrisson H, Nordquist J, Walther S, Eriksson LI, and Larsson L**. A porcine model of acute quadriplegic myopathy: a feasibility study. *Acta Anaesthesiol Scand* 50: 1058-1067, 2006.
103. **Nosek TM, Brotto MA, Essig DA, Mestril R, Conover RC, Dillmann WH, and Kolbeck RC**. Functional properties of skeletal muscle from transgenic animals with upregulated heat shock protein 70. *Physiol Genomics* 4: 25-33, 2000.
104. **Ochala J, Gustafson AM, Diez ML, Renaud G, Li M, Aare S, Qaisar R, Banduseela VC, Hedstrom Y, Tang X, Dworkin B, Ford GC, Nair KS, Perera S, Gautel M, and Larsson L**. Preferential skeletal muscle myosin loss in response to mechanical silencing in a novel rat intensive care unit model: underlying mechanisms. *J Physiol* 589: 2007-2026, 2011.
105. **Okamoto K, Wang W, Rounds J, Chambers E, and Jacobs DO**. Sublytic complement attack increases intracellular sodium in rat skeletal muscle. *J Surg Res* 90: 174-182, 2000.
106. **Ooi PT, da Costa N, Edgar J, and Chang KC**. Porcine congenital splayleg is characterised by muscle fibre atrophy associated with relative rise in MAFbx and fall in P311 expression. *BMC Vet Res* 2: 23, 2006.
107. **Pette D, and Staron RS**. Cellular and molecular diversities of mammalian skeletal muscle fibers. *Rev Physiol Biochem Pharmacol* 116: 1-76, 1990.
108. **Polla B, D'Antona G, Bottinelli R, and Reggiani C**. Respiratory muscle fibres: specialisation and plasticity. *Thorax* 59: 808-817, 2004.

109. **Puente LG, Voisin S, Lee RE, and Megeney LA**. Reconstructing the regulatory kinase pathways of myogenesis from phosphopeptide data. *Mol Cell Proteomics* 5: 2244-2251, 2006.
110. **Radell PJ, Remahl S, Nichols DG, and Eriksson LI**. Effects of prolonged mechanical ventilation and inactivity on piglet diaphragm function. *Intensive Care Med* 28: 358-364, 2002.
111. **Raffaello A, Milan G, Masiero E, Carnio S, Lee D, Lanfranchi G, Goldberg AL, and Sandri M**. JunB transcription factor maintains skeletal muscle mass and promotes hypertrophy. *J Cell Biol* 191: 101-113, 2010.
112. **Reconditi M, Koubassova N, Linari M, Dobbie I, Narayanan T, Diat O, Piazzesi G, Lombardi V, and Irving M**. The conformation of myosin head domains in rigor muscle determined by X-ray interference. *Biophys J* 85: 1098-1110, 2003.
113. **Richard I, Broux O, Allamand V, Fougerousse F, Chiannilkulchai N, Bourg N, Brenguier L, Devaud C, Pasturaud P, Roudaut C, and et al.** Mutations in the proteolytic enzyme calpain 3 cause limb-girdle muscular dystrophy type 2A. *Cell* 81: 27-40, 1995.
114. **Rommel C, Bodine SC, Clarke BA, Rossman R, Nunez L, Stitt TN, Yancopoulos GD, and Glass DJ**. Mediation of IGF-1-induced skeletal myotube hypertrophy by PI(3)K/Akt/mTOR and PI(3)K/Akt/GSK3 pathways. *Nat Cell Biol* 3: 1009-1013, 2001.
115. **Rouleau G, Karpati G, Carpenter S, Soza M, Prescott S, and Holland P**. Glucocorticoid excess induces preferential depletion of myosin in denervated skeletal muscle fibers. *Muscle Nerve* 10: 428-438, 1987.
116. **Rudis MI, Guslits BJ, Peterson EL, Hathaway SJ, Angus E, Beis S, and Zarowitz BJ**. Economic impact of prolonged motor weakness complicating neuromuscular blockade in the intensive care unit. *Crit Care Med* 24: 1749-1756, 1996.
117. **Sackey PV, Martling CR, Granath F, and Radell PJ**. Prolonged isoflurane sedation of intensive care unit patients with the Anesthetic Conserving Device. *Crit Care Med* 32: 2241-2246, 2004.
118. **Sambasivan R, Gayraud-Morel B, Dumas G, Cimper C, Paisant S, Kelly RG, and Tajbakhsh S**. Distinct regulatory cascades govern extraocular and pharyngeal arch muscle progenitor cell fates. *Dev Cell* 16: 810-821, 2009.
119. **Sander HW, Golden M, and Danon MJ**. Quadriplegic areflexic ICU illness: selective thick filament loss and normal nerve histology. *Muscle Nerve* 26: 499-505, 2002.
120. **Sandri M, Sandri C, Gilbert A, Skurk C, Calabria E, Picard A, Walsh K, Schiaffino S, Lecker SH, and Goldberg AL**. Foxo transcription factors induce the atrophy-related ubiquitin ligase atrogin-1 and cause skeletal muscle atrophy. *Cell* 117: 399-412, 2004.
121. **Schiaffino S, and Reggiani C**. Fiber types in mammalian skeletal muscles. *Physiol Rev* 91: 1447-1531, 2011.
122. **Schiaffino S, and Reggiani C**. Molecular diversity of myofibrillar proteins: gene regulation and functional significance. *Physiol Rev* 76: 371-423, 1996.
123. **Schiaffino S, and Reggiani C**. Myosin isoforms in mammalian skeletal muscle. *J Appl Physiol* 77: 493-501, 1994.
124. **Segredo V, Caldwell JE, Matthay MA, Sharma ML, Gruenke LD, and Miller RD**. Persistent paralysis in critically ill patients after long-term administration of vecuronium. *N Engl J Med* 327: 524-528, 1992.
125. **Seneff MG, Wagner D, Thompson D, Honeycutt C, and Silver MR**. The impact of long-term acute-care facilities on the outcome and cost of care for

patients undergoing prolonged mechanical ventilation. *Crit Care Med* 28: 342-350, 2000.
126. **Senf SM, Dodd SL, and Judge AR**. FOXO signaling is required for disuse muscle atrophy and is directly regulated by Hsp70. *Am J Physiol Cell Physiol* 298: C38-45.
127. **Senf SM, Dodd SL, and Judge AR**. FOXO signaling is required for disuse muscle atrophy and is directly regulated by Hsp70. *Am J Physiol Cell Physiol* 298: C38-45, 2010.
128. **Setsuie R, Suzuki M, Tsuchiya Y, and Wada K**. Skeletal muscles of Uchl3 knockout mice show polyubiquitinated protein accumulation and stress responses. *Neurochem Int* 56: 911-918.
129. **Shah OJ, Kimball SR, and Jefferson LS**. Acute attenuation of translation initiation and protein synthesis by glucocorticoids in skeletal muscle. *Am J Physiol Endocrinol Metab* 278: E76-82, 2000.
130. **Shah OJ, Kimball SR, and Jefferson LS**. Glucocorticoids abate p70(S6k) and eIF4E function in L6 skeletal myoblasts. *Am J Physiol Endocrinol Metab* 279: E74-82, 2000.
131. **Shee CD**. Risk factors for hydrocortisone myopathy in acute severe asthma. *Respir Med* 84: 229-233, 1990.
132. **Singh BN, Rao KS, Ramakrishna T, Rangaraj N, and Rao Ch M**. Association of alphaB-crystallin, a small heat shock protein, with actin: role in modulating actin filament dynamics in vivo. *J Mol Biol* 366: 756-767, 2007.
133. **Singh BN, Rao KS, and Rao Ch M**. Ubiquitin-proteasome-mediated degradation and synthesis of MyoD is modulated by alphaB-crystallin, a small heat shock protein, during muscle differentiation. *Biochim Biophys Acta* 1803: 288-299.
134. **Siu PM, and Alway SE**. Mitochondria-associated apoptotic signalling in denervated rat skeletal muscle. *J Physiol* 565: 309-323, 2005.
135. **Smuder AJ, Kavazis AN, Hudson MB, Nelson WB, and Powers SK**. Oxidation enhances myofibrillar protein degradation via calpain and caspase-3. *Free Radic Biol Med* 49: 1152-1160.
136. **Smyth GK**. Linear models and empirical bayes methods for assessing differential expression in microarray experiments. *Stat Appl Genet Mol Biol* 3: Article3, 2004.
137. **Sturn A, Quackenbush J, and Trajanoski Z**. Genesis: cluster analysis of microarray data. *Bioinformatics* 18: 207-208, 2002.
138. **Supinski GS, and Callahan LA**. Diaphragmatic free radical generation increases in an animal model of heart failure. *J Appl Physiol* 99: 1078-1084, 2005.
139. **Tateyama M, Fujihara K, Misu T, Feng J, Onodera Y, and Itoyama Y**. Expression of CCR7 and its ligands CCL19/CCL21 in muscles of polymyositis. *J Neurol Sci* 249: 158-165, 2006.
140. **Tessier SN, and Storey KB**. Expression of myocyte enhancer factor-2 and downstream genes in ground squirrel skeletal muscle during hibernation. *Mol Cell Biochem* 344: 151-162, 2010.
141. **Thirion C, Stucka R, Mendel B, Gruhler A, Jaksch M, Nowak KJ, Binz N, Laing NG, and Lochmuller H**. Characterization of human muscle type cofilin (CFL2) in normal and regenerating muscle. *Eur J Biochem* 268: 3473-3482, 2001.
142. **Trendelenburg AU, Meyer A, Rohner D, Boyle J, Hatakeyama S, and Glass DJ**. Myostatin reduces Akt/TORC1/p70S6K signaling, inhibiting

myoblast differentiation and myotube size. *Am J Physiol Cell Physiol* 296: C1258-1270, 2009.
143. **Tsai S, Cassady JP, Freking BA, Nonneman DJ, Rohrer GA, and Piedrahita JA**. Annotation of the Affymetrix porcine genome microarray. *Anim Genet* 37: 423-424, 2006.
144. **Wang K, Wang C, Xiao F, Wang H, and Wu Z**. JAK2/STAT2/STAT3 are required for myogenic differentiation. *J Biol Chem* 283: 34029-34036, 2008.
145. **Wang X, Blagden C, Fan J, Nowak SJ, Taniuchi I, Littman DR, and Burden SJ**. Runx1 prevents wasting, myofibrillar disorganization, and autophagy of skeletal muscle. *Genes Dev* 19: 1715-1722, 2005.
146. **Widmer CG, Morris-Wiman JA, and Nekula C**. Spatial distribution of myosin heavy-chain isoforms in mouse masseter. *J Dent Res* 81: 33-38, 2002.
147. **Vyas DR, Spangenburg EE, Abraha TW, Childs TE, and Booth FW**. GSK-3beta negatively regulates skeletal myotube hypertrophy. *Am J Physiol Cell Physiol* 283: C545-551, 2002.
148. **Yu F, Stal P, Thornell LE, and Larsson L**. Human single masseter muscle fibers contain unique combinations of myosin and myosin binding protein C isoforms. *J Muscle Res Cell Motil* 23: 317-326, 2002.
149. **Zergeroglu MA, McKenzie MJ, Shanely RA, Van Gammeren D, DeRuisseau KC, and Powers SK**. Mechanical ventilation-induced oxidative stress in the diaphragm. *J Appl Physiol* 95: 1116-1124, 2003.
150. **Zink W, Kollmar R, and Schwab S**. Critical illness polyneuropathy and myopathy in the intensive care unit. *Nat Rev Neurol* 5: 372-379, 2009.

Acta Universitatis Upsaliensis

Digital Comprehensive Summaries of Uppsala Dissertations from the Faculty of Medicine 812

Editor: The Dean of the Faculty of Medicine

A doctoral dissertation from the Faculty of Medicine, Uppsala University, is usually a summary of a number of papers. A few copies of the complete dissertation are kept at major Swedish research libraries, while the summary alone is distributed internationally through the series Digital Comprehensive Summaries of Uppsala Dissertations from the Faculty of Medicine.

Distribution: publications.uu.se
urn:nbn:se:uu:diva-180374

ACTA
UNIVERSITATIS
UPSALIENSIS
UPPSALA
2012